EFFECT OF SEVERE PLASTIC DEFORMATION ON MECHANICAL PROPERTIES OF WELDED ST37-2 STEEL

Abubaker H. Almabruk SAHHAL

2020
PhD THESIS
MECHANICAL ENGINEERING

Thesis Advisor
Prof. Dr. Mustafa GÜNAY

EFFECT OF SEVERE PLASTIC DEFORMATION ON MECHANICAL PROPERTIES OF WELDED ST-37-2 STEEL

Abubaker H. Almabruk SAHHAL

T.C.
Karabuk University
Institute of Graduate Programs
Department of Mechanical Engineering
Prepared as
Doctor of Philosophy

Thesis Advisor
Prof. Dr. Mustafa GÜNAY

KARABÜK
December 2020

I certify that in my opinion the thesis submitted by Abubaker SAHHAL titled "EFFECT OF SEVERE PLASTIC DEFORMATION ON MECHANICAL PROPERTIES OF WELDED ST37-2 STEEL" is fully adequate in scope and in quality as a thesis for the degree of Doctor of Philosophy of science.

Prof. Dr. ……
Thesis Advisor, Department of Mechanical Engineering

This thesis is accepted by the examining committee with a unanimous vote in the Department of Mechanical Engineering as a Doctor of philosophy thesis. XX/XX/2020

Examining Committee Members (Institutions)	Signature
Chairman: Associate. Prof. Dr.	……
Member : Prof. Dr. Mustafa GÜNAY (KBU)	……
Member : Associate. Prof. Dr.	……
Member : Asist. Prof. Dr.	……
Member : Asist. Prof. Dr.	……

The degree of Doctor of Philosophy by the thesis submitted is approved by the Administrative Board of the Institute of Graduate Programs, Karabuk University.

Prof. Dr. Hasan SOLMAZ ……
Director of the Institute of Graduate Programs

"I declare that all the information within this thesis has been gathered and presented in accordance with academic regulations and ethical principles and I have according to the requirements of these regulations and principles cited all those which do not originate in this work as well"

Abubaker SAHHAL

ABSTRACT

Ph.D. Thesis

EFFECT OF SEVERE PLASTIC DEFORMATION ON MECHANICAL PROPERTIES OF WELDED ST37-2 STEEL

Abubaker H. Almabruk SAHHAL

Karabük University
Institute of Graduate Programs
The Department of Mechanical Engineering

Thesis Advisor:
Prof. Dr. Mustafa GÜNAY
December 2020, 77 pages

Cold treatment techniques are used to enhance the mechanical properties of metal alloys, while the most important characteristics are strength, roughness and microstructure. Severe plastic deformation (SPD) is formed in metals through processes, such as hydrostatic extrusion, which performs deformations in the metal at low temperatures, in comparison with other techniques. SPD results into a fine crystalline structure, that differs from the crystallographic structure of the original metal or alloy, through forming micrometric and submicrometric sub-grains in the coarse grain of the original material. SPD comes with different advantages and disadvantages that are related to the mechanical properties and performance of the material.

ST37-2 is a low carbon mild steel that is mostly used as a structural metal due to several performance criteria it possesses. The alloy has excellent weldability and

good ductility, which qualified it to be used in many applications, including shelters and water vessels, and can be shaped for several purposes as angles, strips, sheets, and plates. ST37-2 is non-alloy in its standard form processed through hot rolling.

The aim of the research is to test the effect of conventional shot peening (CSP) and severe shot peening (SSP) on the mechanical properties of ST37-2 steel. The results of the experiment showed enhancements in surface roughness and tensile strength. However, shot peening decreased the ductility of the metal and caused changes in its microstructure that are indicated in the XRF and XRD tests. Data are provided for ST37-2 steel, as an original contribution to the literature, while comparing results with existing data. The tensile strength values indicate enhancements in yield strength and ultimate tensile strength values reaching up to 19.7% and 22.8% with CSP and SSP, respectively, while elongation decreased up to 27.2%, confirming the decrease in ductility with shot peening. Hardness of the alloy increased in treated samples, as well as changes in microstructure are indicated through XRF and XRD analyses. Deformation intensities are increased, as investigated through optical microscopy, while the layer thickness increase in the SSP case, in comparison with the CSP case, is observed in the FESEM study.

Keywords **:** Low carbon steel, ST37-2, Shot peening, Arc welding, Severe plastic deformation

Science Code : 91421

ÖZET

Doktora Tezi

ŞİDDELİ PLASTİK DEFORMASYONUN KAYNAKLI ST37-2 ÇELİĞİN MEKANİK ÖZELLİKLERİ ÜZERİNE ETKİSİ

Abubaker H. Almabruk SAHHAL

Karabük Üniversitesi
Lisansüstü Eğitim Enstitüsü
Makine Mühendisliği

Tez Danışmanı:
Prof. Dr. Mustafa GÜNAY
Aralık 2020, 77 sayfa

Metal alaşımlarının mekanik özelliklerini geliştirmek için soğuk işlem teknikleri kullanılırken, en önemli özellikler mukavemet, pürüzlülük ve mikroyapıdır. Diğer tekniklere göre düşük sıcaklıklarda metalde deformasyon gerçekleştiren hidrostatik ekstrüzyon gibi işlemlerle metallerde ciddi plastik deformasyon (SPD) oluşur. SPD, orijinal malzemenin iri taneciklerinde mikrometrik ve mikrometrik alt tanecikler oluşturarak orijinal metal veya alaşımın kristalografik yapısından farklı olan ince bir kristal yapıya neden olur. SPD, malzemenin mekanik özellikleri ve performansı ile ilgili farklı avantaj ve dezavantajlarla birlikte gelir.

ST37-2, sahip olduğu çeşitli performans kriterleri nedeniyle çoğunlukla yapısal metal olarak kullanılan düşük karbonlu yumuşak bir çeliktir. Alaşım, mükemmel kaynaklanabilirliğe ve iyi sünekliğe sahiptir, bu da onu barınaklar ve su tankları dahil olmak üzere birçok uygulamada kullanılmak üzere nitelendirir ve açılar, şeritler,

levhalar ve plakalar gibi çeşitli amaçlarla şekillendirilebilir. ST37-2, sıcak haddeleme ile işlenmiş standart formda alaşımsızdır.

Araştırmanın amacı, geleneksel bilyeli çekiçlemenin (CSP) ve şiddetli bilyeli çekiçlemenin (SSP) ST37-2 çeliğin mekanik özellikleri üzerindeki etkisini test etmektir. Deneyin sonuçları, yüzey pürüzlülüğünde ve gerilme mukavemetinde gelişmeler gösterdi. Ancak bilye çekiçleme, metalin sünekliğini azaltmış ve mikro yapısında XRF ve XRD testlerinde belirtilen değişikliklere neden olmuştur. Veriler, sonuçlar mevcut verilerle karşılaştırılırken, literatüre orijinal bir katkı olarak ST37-2 çeliğine yönelik olarak sağlanır. Çekme mukavemeti değerleri, CSP ve SSP ile akma dayanımı ve nihai gerilme mukavemeti değerlerinde sırasıyla% 19,7 ve% 22,8'e ulaşan artışları gösterirken, uzama% 27,2'ye kadar düşerek bilyeli çekiçlemeyle süneklikteki azalmayı teyit etmektedir. İşlem görmüş numunelerde alaşımın sertliği arttığı gibi mikroyapıda meydana gelen değişiklikler XRF ve XRD analizleri ile gösterilir. Optik mikroskopi ile incelendiği üzere deformasyon yoğunlukları artarken, FESEM çalışmasında CSP vakasına göre SSP vakasında tabaka kalınlığının arttığı gözlemlenmiştir.

Anahtar Kelimeler : Düşük karbonlu çelik, St37-2, Bilyalı dövme; Ark kaynağı, Şiddetli plastik deformasyon.

Bilim Kodu **:** 91421

ACKNOWLEDGMENTS

My greatest gratitude to God the almighty for enabling me to complete my research and studies, despite the difficulties and the challenges.

I attribute this research to my supervisor Prof. Dr. Mustafa Günay and his continuous assistance and encouragement in this journey.

My sincere gratitude to the one who filled us with love and worked hard to provide us with a moment of happiness and pave the way for us towards knowledge: my late father, may God bless his soul.

My sincere gratitude to the one who fed us sympathy and love to the purist heart of all hearts: my beloved late mother, may God bless her soul.

My sincere gratitude to the kind hearts and life companions, my beloved wife and children.

And to all those who stood by me and are close to my heart.

CONTENTS

Page

APPROVAL ii
ABSTRACT iv
ÖZET vi
ACKNOWLEDGMENTS viii
CONTENTS ix
LIST OF FIGURES xi
LIST OF TABLES xiv
SYMBOLS AND ABBREVIATIONS xv

CHAPTER 1 1
INTRODUCTION 1
1.1. RESEARCH BACKGROUND 1
1.2. PROBLEM, SCOPE AND METHODOLOGY 2
1.3. PURPOSE OF THE STUDY AND QUESTIONS 3
1.4. ORGANIZATION OF THE STUDY 4

CHAPTER 2 6
LITERATURE REVIEW 6
2.1. PROPERTIES OF STEEL 6
2.1.1. Atomic and Molecular Properties of Iron and Steel 8
2.1.2. Physical Properties of Steel 10
2.1.3. Mechanical Properties of Steel 11
2.2. STEEL ALLOY SYSTEMS AND DESIGNATION 17
2.3. PROPERTIES OF ST37-2 ALLOY 19
2.4. APPLICATIONS AND METALLURGY OF STEEL ALLOYS 25
2.4.1. Applications of Low Carbon Steel 25
2.4.1.1. Machinery and Vehicles 25
2.4.1.2. Construction and Pipelines 26

Page

2.4.1.3. Tools and Cookware 26
2.4.2. Metallurgical Properties of Steel Alloys 27
2.5. EEFECTS OF ARC WELDING ON STEEL MATERIAL PROPERTIES .. 33
2.6. MECHANISM OF SHOT PEENING 34

CHAPTER 3 40
METHODOLOGY AND EXPERIMENT 40
3.1. MATERIAL 40
3.2. SAMPLE PREPARATION 40
3.3. MICROSTRUCTURAL CHARACTERIZATION AND PHASE ANALYSIS 43
3.4. ROUGHNESS TEST 44
3.5. TENSILE TEST 44
3.6. HARDNESS TEST 45

CHAPTER 4 46
RESULTS AND DISCUSSION 46
4.1. ROUGHNESS TEST 46
4.2. TENSILE TEST 48
4.3. MICROHARDNESS 52
4.4. XRF ANALYSIS 53
4.5. XRD ANALYSIS 54
4.6. OPTICAL MICROSCOPE 54
4.7. SCANNING ELECTRON MICROSCOPY (SEM) OBSERVATIONS 58

CHAPTER 5 60
CONCLUSIONS 60

REFERENCES 62

APPENDIX A. FESEM IMAGES 70
RESUME 77

LIST OF FIGURES

Page

Figure 2.1. Crude steel production in the world over 40 years 8

Figure 2.2. Crystal lattice of steel 9

Figure 2.3. Phase diagram for iron-carbon equilibrium in steel 10

Figure 2.4. Temperature-time schematic graph for steel rolling 12

Figure 2.5. General stress-strain curves for steel before (left) and after (right) heat treatment 13

Figure 2.6. Difference in mechanical properties of steel with heat treatment 14

Figure 2.7. Example of fatigue test results for a comparison between a wrought and cast steel 15

Figure 2.8. Reduction in steel toughness with the increase of carbon content measured through a Charpy V-notch test 16

Figure 2.9. Thermal conductivity of ST37-2 21

Figure 2.10. Mechanical properties of ST37-2 22

Figure 2.11. Thermal expansion coefficient of ST37-2. 22

Figure 2.12. Material used for vehicular structural components 26

Figure 2.13. Microstructure imaging showing acicular and proeutectoid ferrites 28

Figure 2.14. Equilibrium between oxygen and silicon contents in steel with comparison between A and B 29

Figure 2.15. Partial recrystallized steel after 17 hours of annealing 30

Figure 2.16. Impact of temperature on steel crystallization 30

Figure 2.17. Platelets of iron nitride precipitates on steel surface through SEM 31

Figure 2.18. Precipitates of globular vanadium carbide at nanosized scale (dark zones) 32

Figure 2.19. Changes in the profile of residual stress with shot peening 35

Figure 2.20. Relationship between tensile strength of steel and residual stressed induced by shot peeing 36

Figure 2.21. Distribution of residual stress after shot peening 37

Figure 2.22. Residual and applied shot peening stresses at superposition 37

Figure 2.23. Bending stress distribution in notched specimens 38

Figure 2.24. Distribution of stress and load for bending a shot peened specimen 39

Figure 3.1. Arc welding of steel plates. 41

Page

Figure 3.2. Schematic of tested specimens. 41
Figure 3.3. Samples for tensile testing (top) and fatigue testing (bottom). 41
Figure 3.4. Surface of ST37-2 after shot peening; A12-14. 42
Figure 3.5. Surface of ST37-2 after shot peening; A28-30. 43
Figure 3.6. MITUTOYO Surftest 211. 44
Figure 3.7. Zwich/Roell Z600 universal test machine. 44
Figure 3.8. Q10 A+ QNESS microhardness testing machine. 45
Figure 4.1. Roughness test profile for untreated sample. 47
Figure 4.2. Roughness test profile for CSP sample (A12-14). 47
Figure 4.3. Roughness test profile for SSP (A28-30). 47
Figure 4.4. Tensile test plots for untreated samples. 50
Figure 4.5. Tensile test plots for CSP samples. 51
Figure 4.6. Tensile test plot for SSP sample. 52
Figure 4.7. Vickers hardness values of the investigated alloys. 53
Figure 4.8. Diffractogram of XRD analysis. 54
Figure 4.9. Optical microscope images for shot peened CSP A12-14 sample. 55
Figure 4.10. Optical microscope images for shot peened SSP A28-30 sample. 55
Figure 4.11. Additional optical microscopy for CSP samples. 56
Figure 4.12. Additional optical microscopy for SSP samples. 57
Figure 4.13. FESEM images of plastic deformed layer of shot peened specimen: CSP A12-14 (top-layer thickness = 7.8 μm). 58
Figure 4.14. FESEM images of plastic deformed layer of shot peened specimen: SSP A28-30 (bottom-layer thickness = 9.7 μm). 59
Figure A.1. FESEM images and thickness of the plastic deformed layer of shot peened specimens ST 37-2 (Magnification at 3.00 KX). 71
Figure A.2. FESEM images and thickness of the plastic deformed layer of shot peened specimens ST 37-2 (Magnification at 5.00 KX). 71
Figure A.3. FESEM images and thickness of the plastic deformed layer of shot peened specimens ST37-2 (Magnification at 10.00 KX). 72
Figure A.4. FESEM images and thickness of the plastic deformed layer of shot peened specimens ST 37-2 (Magnification at 500 X). 72
Figure A.5. FESEM images and thickness of the plastic deformed layer of shot peened specimen SSP (A28-30) (Magnification at 3.00 KX). 73
Figure A.6. FESEM images and thickness of the plastic deformed layer of shot peened specimen SSP (A28-30) (Magnification at 5.00 KX). 73

Page

Figure A.7. FESEM images and thickness of the plastic deformed layer of shot peened specimen SSP (A28-30) (Magnification at 10.00 KX). 74

Figure A.8. FESEM images and thickness of the plastic deformed layer of shot peened specimen SSP (A28-30) (Magnification at 500 X). 74

Figure A.9. FESEM images and thickness of the plastic deformed layer of shot peened specimen CSP (A12-14) (Magnification at 3.00 KX). 75

Figure A.10. FESEM images and thickness of the plastic deformed layer of shot peened specimen CSP (A12-14) (Magnification at 5.00 KX). 75

Figure A.11. FESEM images and thickness of the plastic deformed layer of shot peened specimen CSP (A12-14) (Magnification at 10.00 KX). 76

Figure A.12. FESEM images and thickness of the plastic deformed layer of shot peened specimen CSP (A12-14) (Magnification at 500 X). 76

LIST OF TABLES

Page

Table 2.1. The increase in Asian production of crude steel. 8

Table 2.2. Steel designation system for different steel types as per SAE/ AISI standards. 18

Table 2.3. Designations of ST37-2 under different standards 20

Table 2.4. Maximum or minimum limits on the chemical composition of ST37-2 according to British and American standards 20

Table 2.5. Comparison of mechanical properties of ST37-2 between BS and ASTM 21

Table 2.6. Summary of some of ST37-2 literature and its results 23

Table 2.7. Elements added to steel alloys and the improved performance 27

Table 3.1. Chemical composition of ST37-2 (%). 40

Table 3.2. Conditions of shot peening for CSP (Conventional) and SSP (Severe). .. 42

Table 4.1. Surface roughness values. 46

Table 4.2. Tensile strength test outputs. 48

Table 4.3. Results of tensile strength testing. 49

Table 4.4. Vickers microhardness test values. 52

Table 4.5. XRF analysis for ST37-2. 53

SYMBOLS AND ABBREVIATIONS

SYMBOLS

%wt. : Weight percent

Al_2O_3 : Aluminum oxide

CO_2 : Carbon dioxide

Cs_{max} : Maximum compressive strength

C_V : Charpy V-notch test

d : Shot peeing neutral axis point between compressive and tensile

E : Young's modulus of elasticity

Fe_3C : Iron carbide

FeO : Ferrous oxide/ Slag of wustite

GPa : Gigapascal

h : Hour

J : Joule

Kg : Kilogram

kV : Kilo volt

Lo : Gage length

mA : Milliampere

MPa : Megapascal

N : Normalized

NR : Normalized rolled

PA : Flat welding position (both fillet and butt)

PE : Overhead welding position (butt)

psi : Pound per square inch

Ra : Average surface roughness

Rq : Root mean square average of the profile

Rz : Maximum peak to valley height of the profile

sec : Seconds

SiO_2 : Silicon dioxide

SS : Surface Stress

t/a : Ton per annum

Ts_{max} : Maximum simulated tensile stress

V_4C_3 : Vanadium carbide

W : Watt

α : Alpha

Δ : Delta

ε_T : Ultimate tensile strain

ε_Y : Yield strain

μ : Micro

σ_T : Ultimate tensile strength

σ_Y : Yield strength

ABBREVIATIONS

A.D. : Anno Domino

AISI : American Iron and Steel Institute

ASTM : the American Society for Testing and Materials

B.C. : Before Christ

BCC : Body Centered Cubic

BCT : Body Centered Cubic

BS : British Standards

CEV : Carbon Equivalent Value

CSP : Conventional Shot Peening

ECISS : E-mobility Communication and Information System Structure

EDS : Energy Disruptive Spectroscopy

FCC : Face Centered Cubic

FESEM : Field Emission Scanning Electron Microscopy

ICDD : International Centre for Diffraction Data

QT : Quenching and Tempering

SAE : Society of Automotive Engineers

SEM : Scanning Electron Microscopy

SPD : Severe Plastic Deformation

SSP : Severe Shot Peening

TMR : Thermomechanically-Rolled

UTS : Ultimate Tensile Strength

XRD : X-ray Powder Diffraction

XRF : X-ray Fluorescence

YS : Yield Strength

CHAPTER 1

INTRODUCTION

1.1. RESEARCH BACKGROUND

For over three-thousand years, steel has played a major role in advancing the development of humans. Since its early days of discovery, people were able to utilize steel to create farming tools, utensils, until modern research enabled them to use it for building and machinery construction. Iron, the main composite of steel is considered one of the abundant elements in the earth crust: forming 5% of its weight. The easy and less costly extraction and manufacturing methods, in comparison with other metals, encouraged developers to use it in different domains of development. Additionally, iron has several technical properties that makes it, and its most famous alloy steel, one of the preferred elements to work with [1].

Due to its good weldability and ability to provide high performance in terms of hardness, ductility and strength, low carbon steel is used to manufacture different parts of heavy machinery and vehicles [2]. The usage of low carbon steel in this industry is due to several advantages, including ease of forming, high toughness, cost and strength [3]. Low carbon steel is extensively used in construction as main elements, jointing components, and reinforcements for concrete elements. Various structures are created with low carbon steel, such as transmission towers, rail tracks and industrial buildings. Due to it is ability to be rolled, angles and sections are created with low carbon steel, in addition to sheets and bars [4]. the weight of the tool is reduced with the use of less steel material. Low carbon steel is highly conductive for electricity and heat.

ST37-2 is a low carbon mild steel that is mostly used as a structural metal due to several performance criteria it possesses. The alloy has excellent weldability and

good ductility, which qualified it to be used in many applications, including shelters and water vessels, and can be shaped for several purposes as angles, strips, sheets, and plates.

ST37-2 is a low carbon steel used for structural purposes, and it is also non-alloy in its standard form processed through hot rolling. It has a relative density of 7.85 kg/dm^3, according to volumetric mass calculations.

Surface treatment using cold techniques is widely used to enhance the mechanical properties of the metal alloys [5]. Shot peening is one of these processes that has its impact on the surface roughness, residual stresses, microstructure and folding of the metal [6]. The effects of plastic deformations resulting from welding or shot peening can be beneficial or have adverse effects on its strength and ductility [7]. Severe plastic deformation (SPD) is formed in metals through processes, such as hydrostatic extrusion, which performs deformations in the metal at low temperatures, in comparison with other techniques. SPD results into a fine crystalline structure, that differs from the crystallographic structure of the original metal or alloy, through forming micrometric and submicrometric sub-grains in the coarse grain of the original material [8]. The advantages of SPD on performance and mechanical properties through its ability to achieve deformations in the microstructure through fine grains, which reflects on the performance results of hardness and yield stress to saturation levels [9]. However, SPD disadvantages are embodied mainly in the decreased ductility, decreasing the metal ability to undergo plastic deformation under stress [10].

1.2. PROBLEM, SCOPE AND METHODOLOGY

There were many studies that discussed the positive effects of steel cold treatments, especially shot peening on its mechanical properties [11]. The process of shot peening impose compressive stresses on the surface of the metal, which is faced back with a tensile stress from the inner layers. The status of equilibrium between the two forces creates residual stress that increases the hardness of the metal. Furthermore,

the effect of shot peening eliminates failures caused by stress corrosion and fatigue that originate at the surface of the material and propagates [12].

Several steel types have been tested for the effect of shot peening on them, including stainless steel [13], steel sheets [12], high strength QT CrV steel [6], high strength QT CrMo steel [14], case-hardended CrNiMo steel [15], medium carbon CrNiMo steel [16], Dual-phase steel [17], and many other steel alloys. Nonetheless, the majority of these studies are focused on testing the fatigue resistance, frequently studying the microstructure, and rarely addressing strength criteria. Furthermore, there are almost no studies that tested one of the most used structural steels in many industries, which is ST37-2. Therefore, the current study bridges this gap through studying the effect of different shot peening intensities in ST37-2.

1.3. PURPOSE OF THE STUDY AND QUESTIONS

The main aim of the current research is to test the effect of SPD through electric arc welding and shot peening on the mechanical and microstructure of ST37-2. It is expected for these processes to affect the microstructure and homogeneity of the specimens, which leads to altering their mechanical properties. There are several objectives that are achieved through the course of this research:

- Study the basic processes, physical properties, and mechanical properties of steel, which are potentially affected by cold treatment methods.
- Understand the metallurgy properties of steels, and low carbon steels specifically.
- Study steel classification and designation systems.
- Analyze the mechanical properties and microstructure characterization of ST37-2, and its equivalent in different standards, through surveying the literature for studies that provided experimental data, descriptions and findings on the studied alloy.
- Understand the shot peening mechanism and assess its impact on the surface properties of the affected metal, as well as the impact on the internal layers and their reaction to the treatment.

- Provide a review of the most significant applications of low carbon steels, in addition to their advantages and disadvantages.
- Prepare ST37-2 samples with permanent plastic deformations through cutting and welding, in addition to the application of two types of shot peening: one shot peening type for each sample.
- Assess the mechanical properties through a series of tests for tensile strength, toughness, and hardness.
- Assess the microstructure characterization by Scanning Electron Microscopy (SEM) and optical image microscope, in addition to chemical composition using Energy Disruptive Spectroscopy (EDS).
- Analyse the obtained tested results and discuss their implications in conjunction with the results of similar literature.

1.4. ORGANIZATION OF THE STUDY

The research is primarily divided into two main parts: theoretical framework and literature review, and experimental application. For the fulfilment of these parts, the thesis is divided into five chapters:

- Introduction: a brief review of the research subject is carried out, and the research problem, scope and used methodology is identified for further development of the study. Thereafter, the main aim of the study, as well as the objective of each research phase are provided.
- Literature review: a study of the history of iron and steel mining, production, and manufacturing, followed by two sections focusing on the physical and mechanical properties of carbon steels, in addition to the metallurgical properties of steels and their alloys. The designation systems used to identity each steel type with a unique number is provided for further understanding. A review of the literature is performed to cover studies that included ST37-2 in their experiments. A section is provided on shot peening and its mechanism. Finally, a section on the applications of low carbon steels is provided to understand their advantages and disadvantages.

- Methodology and experiment: the chapter provides the steps that were taken to prepare the samples for the experiments, in addition to the procedures and equipment that were used in the different tests.
- Results and discussion: the results of the experiments are provided, along with a comparison and discussion in alignment with the findings of previous literature.
- Conclusions: a summary of the research is carried out, the final results of the experiment are reviewed, and recommendations for future research are given for further development.

CHAPTER 2

LITERATURE REVIEW

2.1. PROPERTIES OF STEEL

For over 3286 years, steel has made a major contribution to human development, e.g., in tools for cultivating the soil and processing stone and almost all other materials, as a construction material for steel and reinforced concrete structures, in transport technology, for the generation and distribution of energy, for the fabrication of machinery and equipment (including equipment for the manufacture of plastics), in the household, and in medicine. It remains, for the foreseeable future, by far the most important material for the maintenance and improvement of our quality of life [18].

The outstanding importance of steel is the result of its ready availability and its versatility. The earth's crust contains ca. 5 wt.% iron, making it the fourth most abundant element after oxygen (46%), silicon (28%), and aluminum (8%). Rich deposits of iron ores are available in many parts of the world. Moreover, the free energy required to isolate iron from its oxide ores is less than half of that required for aluminum [18].

The versatility of steel is due to the polymorphism of the iron crystal and its ability to alloy with other elements, forming solid solutions or compounds. The microstructure of steel in a finished component can be adjusted by means of the chemical composition, the forming conditions, and a wide variety of possible heat treatments. The attainable tensile strength ranges from ca. 300 N/mm^2 for deep drawing sheet steel (e.g., for automotive body parts that are difficult to draw) to >2000 N/mm^2 for critical components in aircraft. Tensile strengths as high as 2600 N/mm^2 are achieved in 0.15 mm diameter drawn wire for steel cord used in radial tires [19].

Cryogenic steels with high strength and good toughness at very low temperatures are used for the transport and storage of liquefied gases at temperatures of ≤ 200 °C. Other steels with good properties at temperatures of 650 – 700 °C and above are used in power station equipment and gas turbines [20].

Highly developed soft magnetic steels are essential in the construction of transformers. Steel is also used to make permanent magnets. Non-magnetizable steels have also been developed for use in electrical technology, shipbuilding, and physics research. Wear-resistant steels are used in rock-crushing machines and in industrial stirring equipment. Machine tools, used for metal cutting, re-quire steels of the highest possible hardness to endow stability to the cutting edge. Other steels with very good machinability have been developed and are used for the economic manufacture of complex turned parts, or for mass production on high-speed automated equipment. Chemically resistant steels are essential in the chemical and foods industries, as well as in household equipment. For the majority of steel grades – more than 2500 are available today – very good welding properties are important, and here steel has an advantage over competing materials [1].

Modern knowledge of controlling the micro-structure of steel, and hence its properties, offer opportunities to match steel products to new sets of requirements [1].

Unlike brick or concrete buildings, steel structures can be dismantled relatively easily. Furthermore, almost 100 % of the steel can be re-covered from steel-containing products and can be re-melted to yield steels of similar or higher quality. In this respect, iron and steel are superior to all competitive materials [1].

The great importance of steel in the world's economy is also exemplified by production figures. In the early 1900s, total world production of steel was less than 3510_6t/a. In 1940, it was $140x10^6$ t/a. The figures for the period after 1950 (Figure 2.1) indicate a surprisingly large growth in world crude steel production after World War II. Up to the mid-1970s, this was mostly due to those developed countries with the greatest rate of economic growth, such as Japan, the six founding countries of the

European Community, and also the former Soviet Union. In the United States, growth had already ceased by the mid-1960s due to market saturation [21].

A rapid increase in steel production also took place in some Latin American countries, continuing until the mid-1980s. In many countries in Asia, Africa, and the Middle East, new steel industries were built up, or existing capacity was increased. The developments in some Asian countries during the last 16 years are remarkable (Table 2.1) [21].

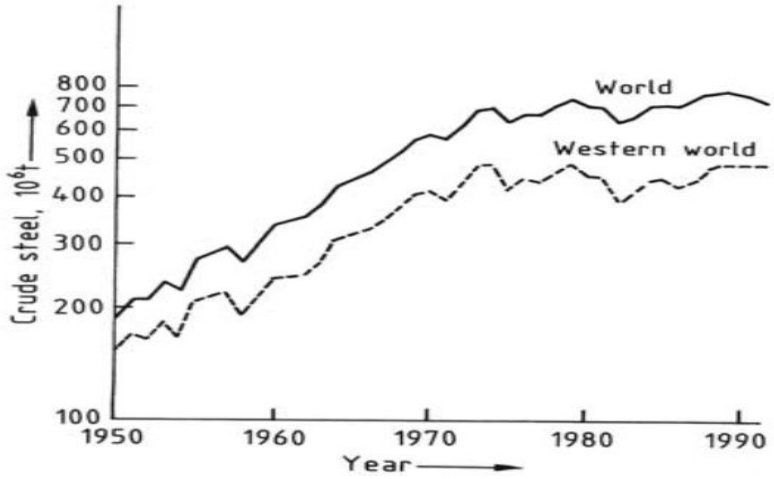

Figure 2.1. Crude steel production in the world over 40 years [21]

Table 2.1. The increase in Asian production of crude steel [21].

Country	Production, 10^3 t/a		
	1975	1985	1995
India	7,991	11,140	17,100
Taiwan	680	5,088	11,000
South Korea	1,994	13,539	26,000
China	23,903	46,700	70,400

2.1.1. Atomic and Molecular Properties of Iron and Steel

Iron is given the symbol Fe in the periodic table and it is a transition metal laying at the eighth group of the periodic table. The atomic number of iron element is 26 and it has an atomic weight of 55.845 g/mol. The element has an equal relative strength in acid-base properties of higher-valence oxides. The atoms interrelate together with a

body-centered cubic crystal structure. The electronic configuration of iron is [Ar] $3d^6 4s^2$ [22].

Steel is an alloy of iron with varying amounts of carbon content (from 0.5 to 1.5%). Steel, being an alloy and therefore not a pure element, is not technically a metal but a variation of one instead which results in them having similar characteristics, thus during this webpage we talk about steel as a metal and explain a lot of steel due to referring to metal. We know that one of the properties of a metal (ex. steel) is that it contains a crystalline structure, which means that the atoms which are in the solid stage are arranged in regular [23], repeating patterns.

The smallest group of atoms which defines the atomic arrangement in a crystal is called the crystal lattice which consist of two forms namely body-centered cubic and face-centered cubic: ferrite and austenite, as shown in Figure 2.2. Steel has three different crystal structures at different temperatures. At room temperature, steel takes the α (alpha) phase with a body centered cubic (BCC) structure. When heated to 913 °C, the structure becomes austenite with a face centered cubic (FCC). When heated to 1394 °C, the steel transforms to the Δ (delta) phase with the structure returning to body centered cubic (BCC). In fast cooling, quenching, the steel returns to the α (alpha) phase and the structure turns into a body centered tetragonal (BCT). Figure 2.3 shows the changes in steel phases according to the carbon content [23].

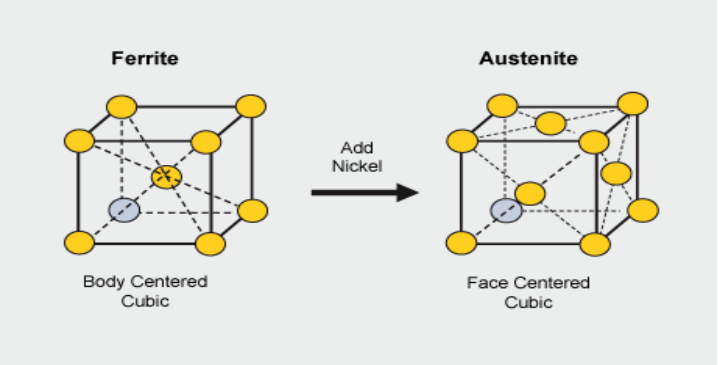

Figure 2.2. Crystal lattice of steel [24].

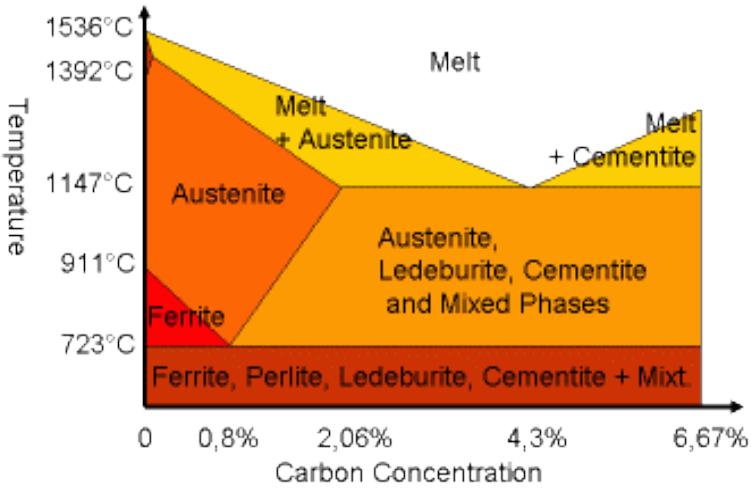

Figure 2.3. Phase diagram for iron-carbon equilibrium in steel [24]

Alloy steel is steel that is alloyed with a variety of "impure" elements in total amounts between 1.0% and 50% by weight. This is done to improve the mechanical property of the steel. Alloy steels are broken down into two groups namely: low-alloy and high-alloy steels. The difference between the two is somewhat arbitrary: Smith and Hashemi [25] define the difference at 4.0%, while DeGarmo, et al. [26], define it at 8.0%. Most commonly, the phrase "alloy steel" refers to low-alloy steels. Strictly speaking, every steel is an alloy, but not all steels are called "alloy steels". The simplest steels are iron (Fe) alloyed with carbon (C) (about 0.1% to 1%, depending on type). However, the term "alloy steel" is the standard term referring to steels with other alloying elements added deliberately in addition to the carbon. The most common alloyants of steel are manganese, nickel, chromium, molybdenum, vanadium, silicon, and boron [24].

2.1.2. Physical Properties of Steel

Steel is a term given to iron with carbon content, as well as a maximum silicon content of 0.5% and maximum manganese content of 1.5%. Therefore, there are four types of carbon steel depending on their carbon content [27]:

- Less than 0.15% carbon content (dead mild steel).
- Between 0.15% to 0.45% carbon content (mild steel or low-carbon steel).

- Between 0.45% to 0.80% carbon content (medium-carbon steel).
- Between 0.80% and 1.50% carbon content (high-carbon steel).

The average density of steel is 7.9 times heavier than water, which makes its relative density 7,900 kg/ m^3. It also has a melting point higher than most metals at 1,510 °C, while pure iron has a melting point of 1,300 °C, copper has melting point of 1,083 °C, nickel has a melting point of 1453 °C, and bronze has a melting point of 1,040 °C. At 20 °C, steel has a linear expansion coefficient of 11.1 μm/m/°C. Therefore, steel has more ability to resist size changes with temperature changes in comparison with other metal, such as lead with 29.1 μm/m/°C, tin with 21.4 μm/m/°C, and copper with 16.7 μm/m/°C [27].

2.1.3. Mechanical Properties of Steel

The variation of the mechanical properties of steel mainly depend on its composition, processing conditions and manufacturing methods. In engineering design, it is essential to understand several aspects of the mechanical properties of steel in order to enable its usage for the suitable elements that can produce the required performance and efficiency. Thus, the understanding of the mechanical properties of steel include its compressive and tensile strengths, toughness, hardness, flexibility, ductility, malleability, and weldability. Other factors affect the mechanical properties of steel, including its heat treatment and the alloyant metals that are used in its composition [28]. The addition of alloys, such as vanadium and manganese, has the ability to increase the strength of steel; however, other properties are negatively affected, such as toughness and ductility [29]. The addition of nickel enhances toughness, while the elimination of Sulphur improves ductility. Due to the high impact of the chemical composition of steel on its mechanical properties, it is crucial to create the most suitable balance between all the elements for the achievement of the desired properties. There is a close connection between the influence of heat treatment and the chemical composition of steel, as well as the mechanical processing techniques that are used during heat treatment [30]. It was found that these factors highly affect all the mechanical properties including strength. The forming and rolling of steel play a major role in its strength, as studies show that

yield strength is reduced with the thickness of the material. There are five main methods of heat treatment that are used for steel: as-rolled, normalized, normalized-rolled, thermomechanically-rolled (TMR) and quenched and tempered (Q&T) [31], as shown in Figure 2.4.

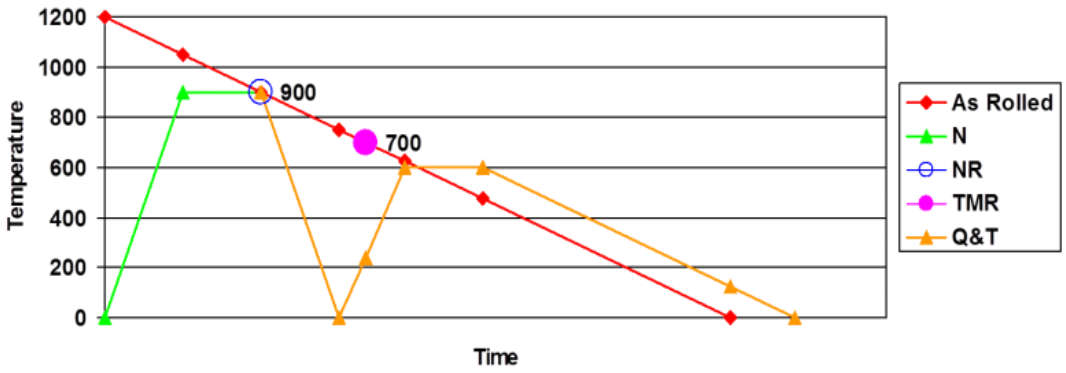

Figure 2.4. Temperature-time schematic graph for steel rolling [31].

When the steel is allowed to cool naturally, after being heated to 1200 °C, it is classified under as-rolled steel. When heated to 900 °C, kept under that temperature for a particular time, then cooled under the room temperature, the steel is classified as normalized, which has enhanced toughness due to the refinement of the grain size. Similarly, the normalized-rolled steel is kept at 900 °C. It is essential to enhance the tensile strength in the steel for a higher performance but without affecting the necessary properties for ductility and toughness, which are best exhibited with low carbon steels that are treated to the finest grains. Such a result can be achieved through TMR steel that is rolled at 700 °C with higher force. When the steel is normalized at 900 °C and quenched/ cooled quickly, a steel with high hardness and strength is produced. Nonetheless, the quenching process reduces the toughness of the steel, which requires the material to be reheated for a maintained temperature of 600 °C and let it naturally reach to room temperature. The previously described process is named quenching and tempering that are used in conjunction to balance hardness, increase strength, and increase the toughness of the steel [31].

The mechanical properties of metals generally, and steel specifically, are presented through several parameters. The general stress-strain curve, shown in Figure 2.5,

demonstrate several indicators for mechanical properties, including: modulus of elasticity (E), yield strength (σ_Y), yield strain (ε_Y), ultimate tensile strength (σ_T) and ultimate tensile strain (ε_T). The figure also shows the ductility caused by the heat treatment and its effect on the elimination of the plastic behavior of the steel [28].

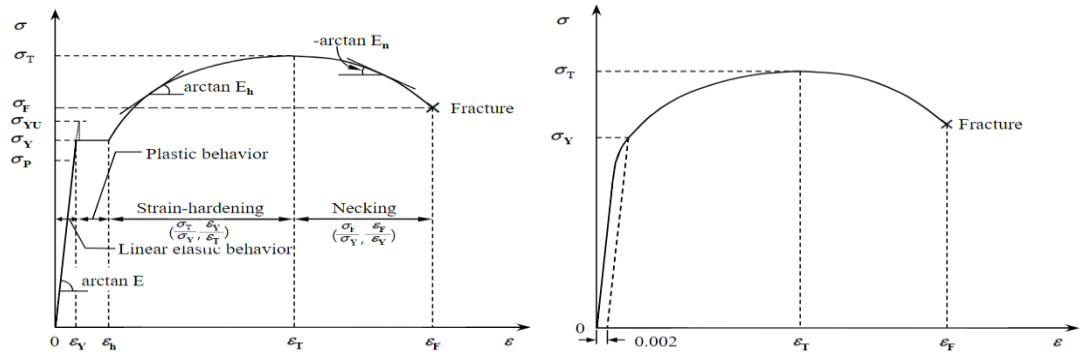

Figure 2.5. General stress-strain curves for steel before (left) and after (right) heat treatment [28].

During the design of engineering elements from steel, ductility, toughness, fatigue, modulus of elasticity and stress values are the most parameters that are focused on. Due to the reverse relationship between the strength and other parameters, it is imperative to balance the requirements of the components to obtain the desired outcomes and know its design limits. The strength of the steel is governed by the amount of load it is able to carry without having any deformations. The yield strength is measured to the extent the component is bearing the load within its elastic range. Thereafter, a permanent and irreversible deformation occurs when this load is exceeded, while the component fractures at the ultimate tensile strength value [30].

The extent of stretching within the component is defined as strain, which is part of the plastic deformation that occurs after exceeding the yield strength. The ductility of the steel is measured through its ability to stretch without cracking during the plastic phase, which decreases with the increase of the strength of the steel. Ductility also depends on the carbon content and the heat treatment of the steel, as shown in Figure 2.6, as increased carbon contents lead to cracks during welding and heat treatment. Based on the results of the tensile test, the modulus of elasticity is derived from the ratio of stress to strain, while heat treatment does not affect the value [32].

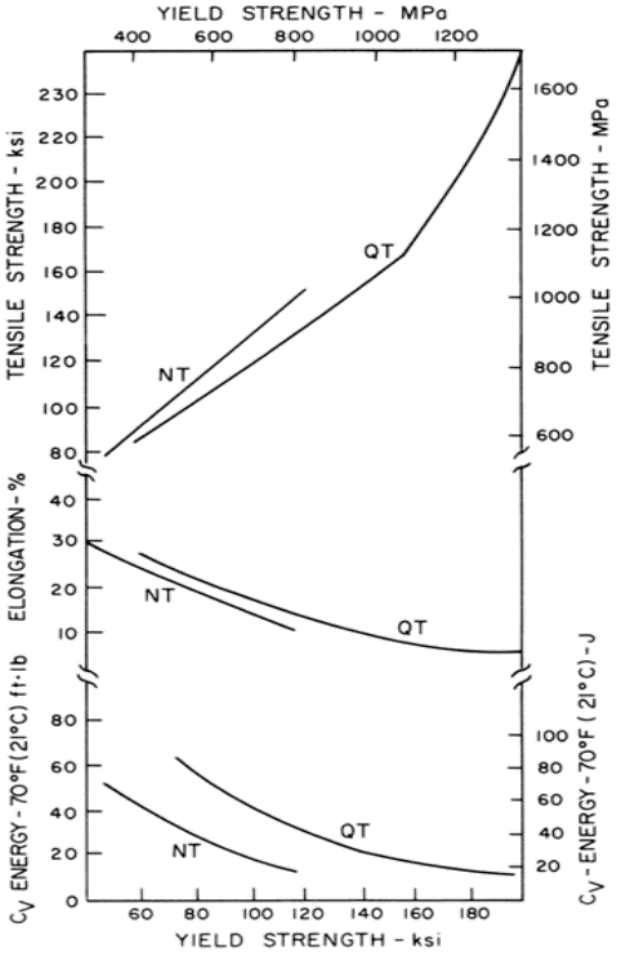

Figure 2.6. Difference in mechanical properties of steel with heat treatment [32].

Despite the failure of the steel component at the yield strength, loading the specimen with repeated smaller loaded can lead to its failure, which is described as fatigue. The parameter is measured through the number of cyclic under a specific load that lead to the failure, as shown in Figure 2.7. The cut off number of loadings is usually at 100,000 cycles. High ductility is needed if the fatigue is below the cut off number of cycles and it is called low cycle fatigue, while high strength is needed if the fatigue id above the cut off number of cycles and it is called high cycle fatigue [32].

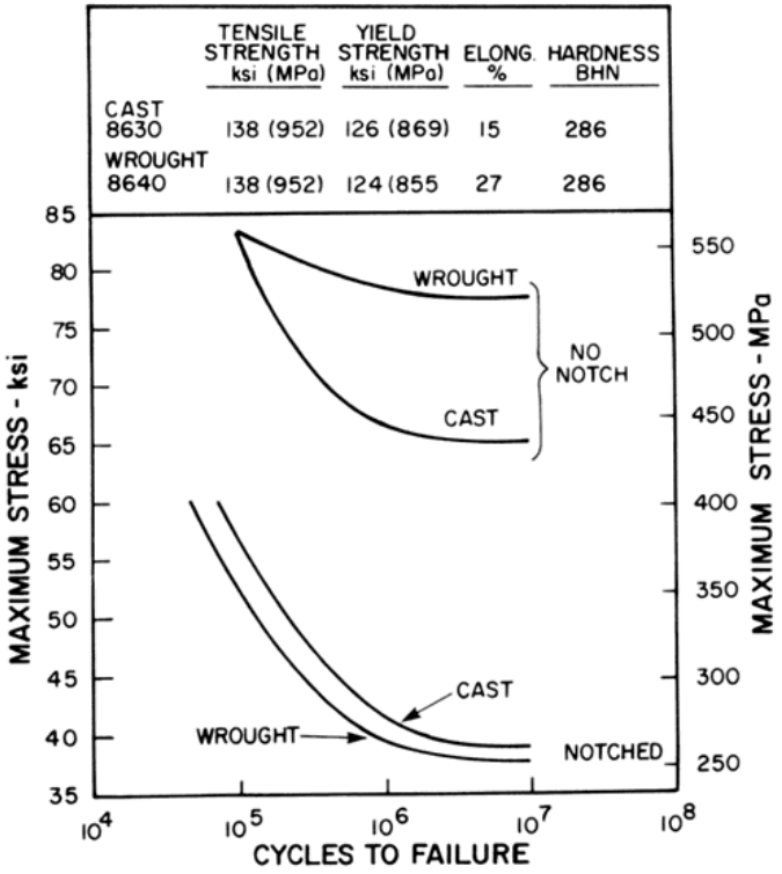

Figure 2.7. Example of fatigue test results for a comparison between a wrought and cast steel [32].

Another mechanical property of steel is its ability to resist impact, which indicates its behavior for cracking or fracture. The parameter measured in this test is the toughness of the steel when it is exposed to impact loadings or low temperatures and able to maintain its integrity without cracking. Therefore, the energy required to cause failure in the steel under s specific temperature is called toughness. For measurement, Charpy test is used to measure toughness, which is in reverse relationship with the strength of the steel specimen. Carbon content is a vital factor in reducing the toughness of the steel. As shown in Figure 2.8, the increase in carbon content of two heat treated steel specimens led to significant reduction in their toughness [33].

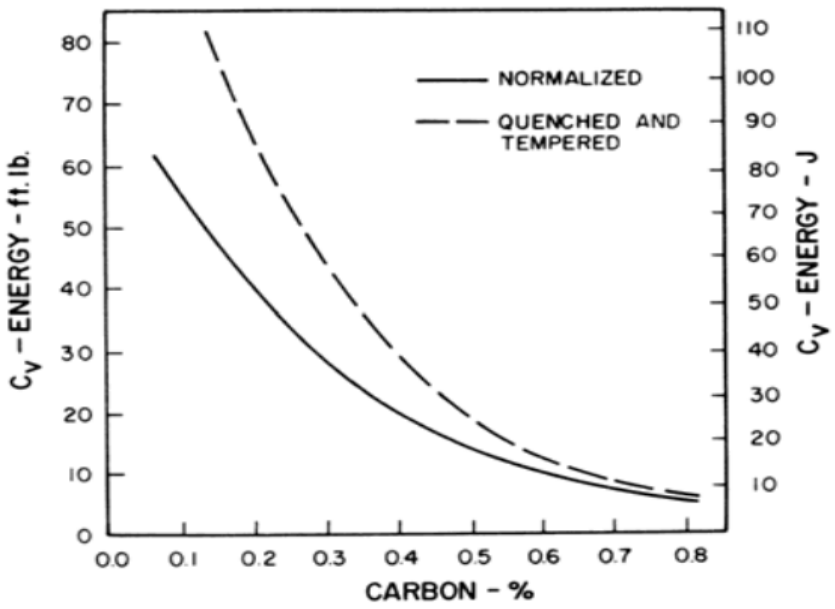

Figure 2.8. Reduction in steel toughness with the increase of carbon content measured through a Charpy V-notch test [33].

The ability of the material to sustain its surface integrity, when rubbed with another material under a specific loading, is measured through a wear test. There are several factors that are considered during the wear test, including corrosion, impact, abrasion and gouging.

The wear test is also a measurement of the steel hardness, as harder steel has the ability to resist wear better than softer counterparts. Steel with higher carbon content and higher strength performs better under the wear test, as these parameters are correlated to increased hardness. The steel has also to have sufficient toughness with high hardness to avoid permanent failure and cracking [34].

Loads below the yield strength value is applied to steel at high temperature to measure its creep, which is its ability to resist stretching permanently under these conditions. Thus, creep is measured as an elongation value with respect to the applied temperature and load, while failure is termed as stress rupture. Generally, steels with higher carbon content and added alloyants have better creep performance. Oxidation is one of the important factors that determine the creep performance of steel, which is also linked to the corrosion behavior of the material. Corrosion tests

can be performed on steel with the application of different weathering conditions, such as oxygen, pH, temperature, and chlorine [34].

2.2. STEEL ALLOY SYSTEMS AND DESIGNATION

Steel alloys are classified and designated through the SAE system, which uses a system of four digits to assign the chemical composition of the alloy. The SAE/ AISI index system, that consists of four digits, have been used since many years and further update in 1995 by the Iron and Steel Society (ISS). The first two digits represent the type of material in the steel alloy composition, while the other two digits represent the percentage of carbon. The system can extend to five digits in some cases, where the three last digits are for the percentage of carbon in the steel.

Carbon steels are designated to the 1XXXX group, and four categories fall under this group:

- 10XX for plain carbon steel with a maximum of 1% manganese
- 11XX for re-sulfurized carbon steel
- 12XX for re-sulfurized and re-phosphorized carbon steel
- 15XX for for high manganese and non-re-sulfurized carbon steel

The first digit in the SAE/ AISI designation system changes based on the main alloyant in its composition, while the second digit represents its percentage:

- 2 for nickel
- 3 for nickel-chromium
- 4 for molybdenum
- 5 for chromium
- 6 for chromium-vanadium
- 7 for tungsten-chromium
- 9 for silicon-manganese

Prefixes and suffixes are added to indicate the following cases:

- XXBXX for added boron between 0.0005% and 0.003%, which is used to improve hardenability.
- XXLXX for added lead between 0.15% and 0.35%, which is used to improve machinability.
- MXXXX for merchant quality steel, which is hot rolled used in non-critical elements.
- EXXXX for electrical-furnace steel
- XXXXH for hardenability requirement

Table 2.2 shows the SAE/ AISI designation system for the different types of steel.

Table 2.2. Steel designation system for different steel types as per SAE/ AISI standards.

Steel Type	SAE/ AISI system	Description
Carbon steels	10XX	Plain carbon, Mn 1.00% max
	11XX	Resulfurized free machining
	12XX	Resulfurized/rephosphorized free machining
	15XX	Plain carbon, Mn 1.00-1.65%
Manganese steels	13XX	Mn 1.75%
Nickel steels	23XX	Ni 3.50%
	25XX	Ni 5.00%
Nickel-chromium steels	31XX	Ni 1.25%, Cr 0.65-0.80%
	32XX	Ni 1.75%, Cr 1.07%
	33XX	Ni 3.50%, Cr 1.50-1.57%
	34XX	Ni 3.00%, Cr 0.77%
Molybdenum steels	40XX	Mo 0.20-0.25%
	44XX	Mo 0.40-0.52%
Chromium-molybdenum steels	41XX	Cr 0.50-0.95%, Mo 0.12-0.30%
Nickel-chromium-molybdenum steels	43XX	Ni 1.82%, Cr 0.50-0.80%, Mo 0.25%
	47XX	Ni 1.05%, Cr 0.45%, Mo 0.20-0.35%
Nickel-molybdenum steels	46XX	Ni 0.85-1.82%, Mo 0.20-0.25%
	48XX	Ni 3.50%, Mo 0.25%
Chromium steels	50XX	Cr 0.27-0.65%
	51XX	Cr 0.80-1.05%
	50XXX	Cr 0.50%, C 1.00% min
	51XXX	Cr 1.02%, C 1.00% min

Steel Type	SAE/ AISI system	Description
	52XXX	Cr 1.45%, C 1.00% min
Chromium-vanadium steels	61XX	Cr 0.60-0.95%, V 0.10-0.015%
Tungsten-chromium steels	72XX	W 1.75%, Cr 0.75%
Nickel-chromium-molybdenum steels	81XX	Ni 0.30%, Cr 0.40%, Mo 0.12%
	86XX	Ni 0.55%, Cr 0.50%, Mo 0.20%
	87XX	Ni 0.55%, Cr 0.50%, Mo 0.25%
	88XX	Ni 0.55%, Cr 0.50%, Mo 0.35%
Silicon-manganese steels	92XX	Si 1.40-2.00%, Mn 0.65-0.85%, Cr 0-0.65%
Nickel-chromium-molybdenum steels	93XX	Ni 3.25%, Cr 1.20%, Mo 0.12%
	94XX	Ni 0.45%, Cr 0.40%, Mo 0.12%
	97XX	Ni 0.55%, Cr 0.20%, Mo 0.20%
	98XX	Ni 1.00%, Cr 0.80%, Mo 0.25%

2.3. PROPERTIES OF ST37-2 ALLOY

ST37-2, also designated as S235JR under European standards (Table 2.3 shows the designations of ST37-2 according to different standards), is a low carbon mild steel that is mostly used as a structural metal due to several performance criteria it possesses. The alloy has excellent weldability and good ductility, which qualified it to be used in many applications, including shelters and water vessels, and can be shaped for several purposes as angles, strips, sheets, and plates. ST37-2 is a low carbon steel used for structural purposes, and it is also non-alloy in its standard form processed through hot rolling. It has a relative density of 7.85 kg/dm^3, according to volumetric mass calculations [35]. Impact strength of ST37-2, and its equivalents, is only checked under special requests from the designers through the deoxidization method, where G1 method is used for rimming steel but the usage of G2 method is not allowed according to British Standards (BS EN 10025). The yield strength of ST37-2 differs according to different standards, where the ASTM standards specify it at 365 MPa for type 1 and a range of 400 MPa to 550 MPa for type 2 [35].

Table 2.3. Designations of ST37-2 under different standards [35].

Standards/ Countries	Designation
EN 10027-1 & ECISS IC 10	S235JR
EN 10027-2	1.0037
EN 10025:1990	FE 360 B
Germany	ST37-2
France	E 24-2
Italy	FE 360 B
Belgium	AE 235-B
Sweden	13 11-00
Portugal	FE 360-B
Norway	NS 12 120

The chemical composition of ST37-2 also differs based on the designating standards. Rahbar and Zakeri [36] performed a chemical composition analysis using a Ladle analysis for a 20 mm specimen of ST37-2 and the results are presented in Table 2.5. Figures 2.9, 2.10 and 2.11 illustrate its thermal conductivity, mechanical properties and thermal expansion coefficient, respectively.

Table 2.4. Maximum or minimum limits on the chemical composition of ST37-2 according to British and American standards [35].

Element	BS EN 10025		ASTM 570/A 570 M-98			
% wt.	Product analysis	Ladle analysis	Type 1	Type2	Heat***	Product***
C *	0.21 at t≤16mm 0.25 at t≤40mm	0.17 at t≤16mm 0.20 at t≤40mm	0.25	0.25	-	-
Mn *	1.5	1.4	0.90	1.35	-	-
Si *	-	-	NR	0.40	-	-
P *	0.055	0.045	0.035	0.035	-	-
S *	0.055	0.045	0.04	0.04	-	-
N *	0.011	0.009	-	-	-	-
Al *	-	-	NR	NR	-	-
Cu	-	-	0.20 **	0.20 **	0.20 *	0.23 *
Ni *	-	-	-	-	0.20	0.23
Cr *	-	-	-	-	0.15	0.19
Mo *	-	-	-	-	0.06	0.07
V *	-	-	-	-	0.008	0.018
Nb *	-	-	-	-	0.008	0.018

*. Maximum % wt. requirement
**. Minimum % wt. requirement
***. For both types 1 & 2
NR = No specified requirement but analysis results should be reported

Table 2.5. Comparison of mechanical properties of ST37-2 between BS and ASTM [35].

Criterion	BS EN 10025			ASTM 570/A 570 M-98		
	Sample & test specifications *		Value	Sample & test specifications *		Value
Minimum yield strength (MPa)	t≤16		235	Type 1 (T1)		250
	16<t≤40		225	Type 2 (T2)		250
Minimum tensile strength (MPa)	t≤3		360 – 510	Type 1 (T1)		Min. 365
	3<t≤100		340 – 470	Type 2 (T2)		400 - 550
Minimum elongation (%)	L_o = 80 mm	t≤1	17	In 50 mm	0.65<t<1.6	17.0 (T1) 16.0 (T2)
		1<t≤1.5	18			
		1.5<t≤2	19		1.6<t<2.5	21.0 (T1) 20.0 (T2)
		2<t≤2.5	20			
		2.5<t≤3	21		2.5<t<6.0	22.0 (T1) 21.0 (T2)
	= 5.6	3<t≤40	26	In 200	2.5<t<6.0	17.0 (T1) 16.0 (T2)

*. Thickness value (t) in mm

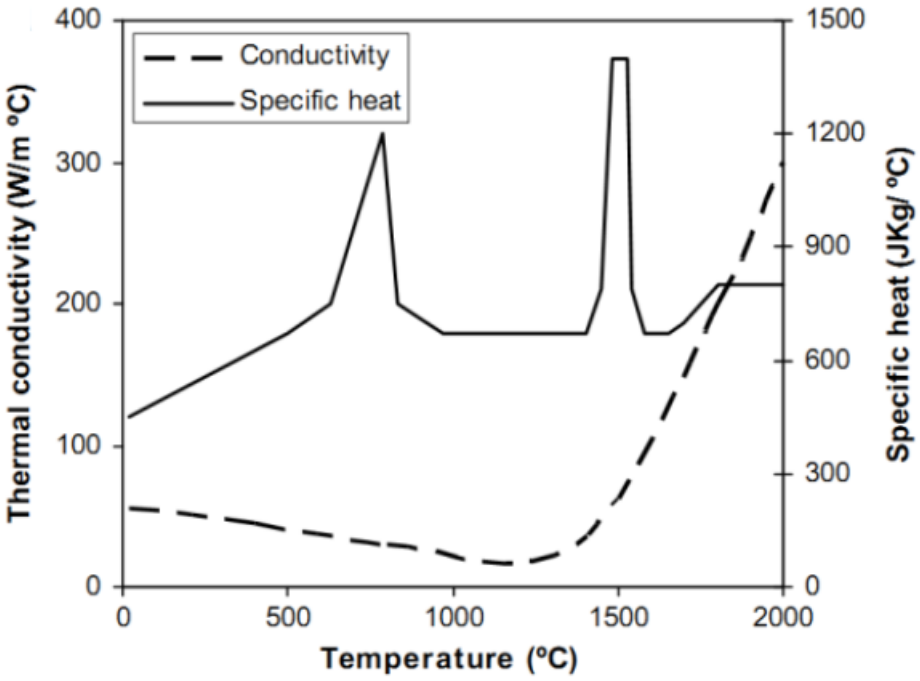

Figure 2.9. Thermal conductivity of ST37-2 [37].

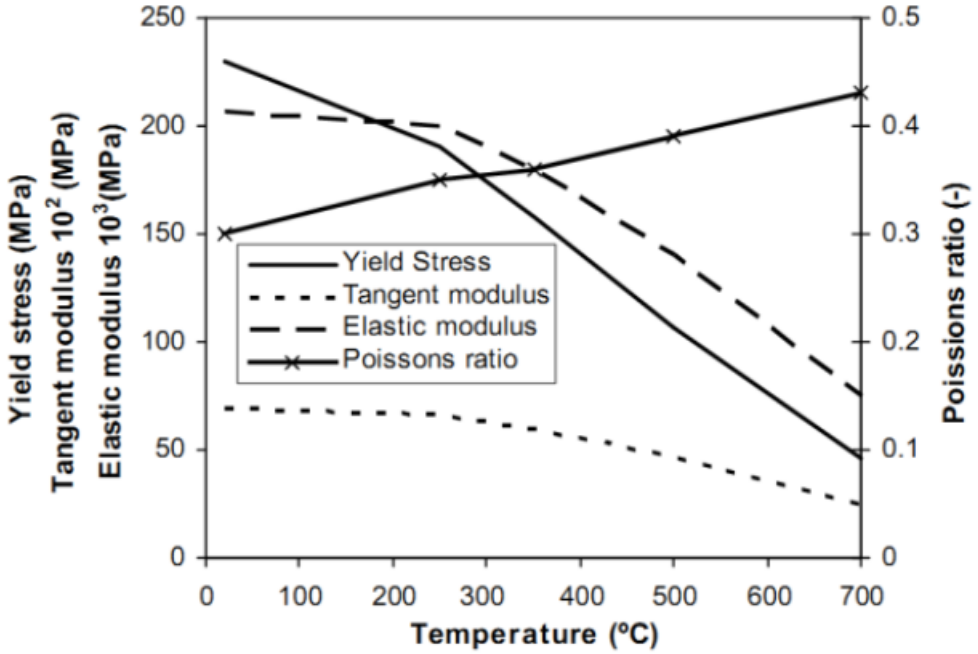

Figure 2.10. Mechanical properties of ST37-2 [37].

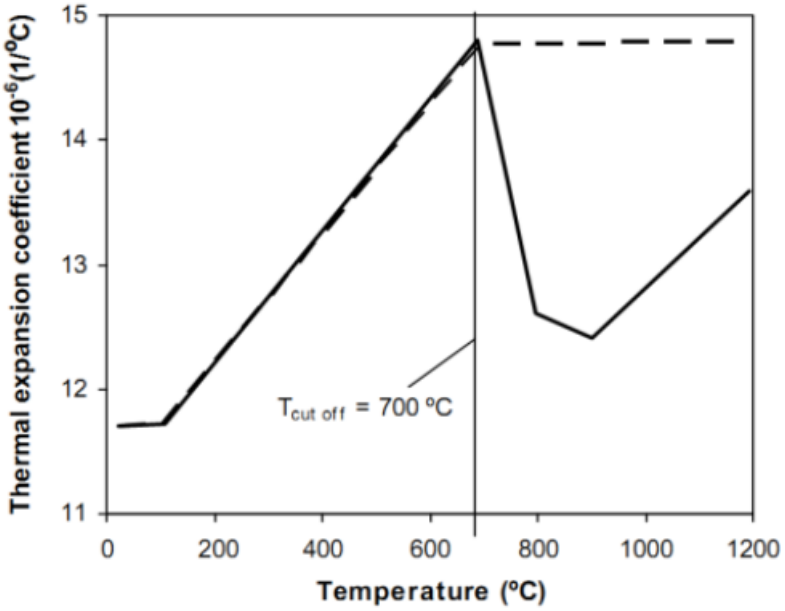

Figure 2.11. Thermal expansion coefficient of ST37-2 [37].

The Carbon Equivalent Value (CEV), carbon content, shape of product, dimensions of product, service conditions and manufacturing conditions are all factors that affect the weldability of carbon steels. Since ST37-2 has less than 0.35% carbon. Therefore, it is considered as a low carbon steel. Due to this carbon content and with

a CEV less than 0.45%, ST37-2 requires no treatment for welding and its weldability is considered to be excellent. If segregation zones are faced in welding, it is recommended that ST37-2 be selected as a rimmed type [35].

Several studies in the literature have experimented with the mechanical and microstructural properties of ST37-2. Depending on the country of origin of the study, the designation used was different from one study to another. However, most of the studies addressed the impact of impact and heat on ST37-2, which are caused by the processing, workmanship and operations performed on it. Table 2.6 provides a summary of the studies that included ST37-2 in their experiments, as well as brief of the outcomes of the research.

Table 2.6. Summary of some of ST37-2 literature and its results.

Author(s)/ Reference	Year	Aim of study	Brief Results
Turcan, et al. [38]	2013	Enhancing hardness of ST37-2 with metallic powder through surface alloying	Hardness enhanced by 500%
Aberkane & Ouali [39]	2011	Measure toughness of ST37-2	A linear relationship is established between the ligament length and total specific work of fracture. Crack length resulting from the experiment is used to calculate essential work of fracture
Djebali, et al. [40]	2015	Measure essential work of fracture for ST37-2	Deformation measured at different points in the sample. At zero ligament length, essential work of fracture is measured as 191.6 kJ/m^2, which a minimum value reaching to 80%
Ebrahimnia, et al. [41]	2009	Study changes in weld properties of ST37-2 with the change of composition of shield gas	Initial increase in absorbed energy with the increase of CO_2, then remained constant with the increase. The increase in CO_2 simulated increase in

Author(s)/ Reference	Year	Aim of study	Brief Results
			acicular ferrite, decrease in inclusions, and increase in fusion zone depth
Turcan, et al. [42]	2014	Enhancing hardness of ST37-2 with CO_2 laser surface treatment	Increase in hardness and penetration depth with the increase of laser speed. Increase of affected depth with the increase in laser power intensity
Chhabra & Bansal [43]	2016	Mig/Mag weld on ST37-2 tested for hardness and penetration with the change in shield gas mix	With the increase of CO2 concentration in the shield gas: toughness initially increased then remained constant, hardness decreased, penetration depth increased, oxygen content increased, increase in YS and UTS up to 4% O_2 and decreased at 5%
Rakhmetov, et al. [44]	2018	Measure fatigue in ST37-2	Degradation of ferrite grains of ST37-2 with dislocation
Sonmez & Ceyhun [45]	2014	Study microstructure and mechanical properties of ST37-2 with welding	Higher hardness values at the PA position and higher tensile strength at the PE position with 600 MPa at the whole mount. Impact energy was the highest at the PA position. Acicular ferrite formation at depth caused by fast cooling.

2.4. APPLICATIONS AND METALLURGY OF STEEL ALLOYS

2.4.1. Applications of Low Carbon Steel

2.4.1.1. Machinery and Vehicles

Due to its good weldability and ability to provide high performance in terms of hardness, ductility and strength, low carbon steel is used to manufacture different parts of heavy machinery and vehicles [2]. Figure 2.12 shows the different parts that are manufactured out of low carbon steel or mild steel for vehicles. The usage of low carbon steel in this industry is due to several advantages [3]:

- The easiness to shape carbon steel into the different panels used for to assemble the vehicle.
- The higher toughness and ductility associated with the low carbon content.
- Low carbon steel is economically feasible especially for mass manufacturing
- High tensile strength providing the necessary strength for structural components of the vehicle.

Poor corrosion resistance is the disadvantage of low carbon steel. Therefore, using it in machinery and vehicle manufacturing requires protecting it with paint coating to separate it from weather conditions [46].

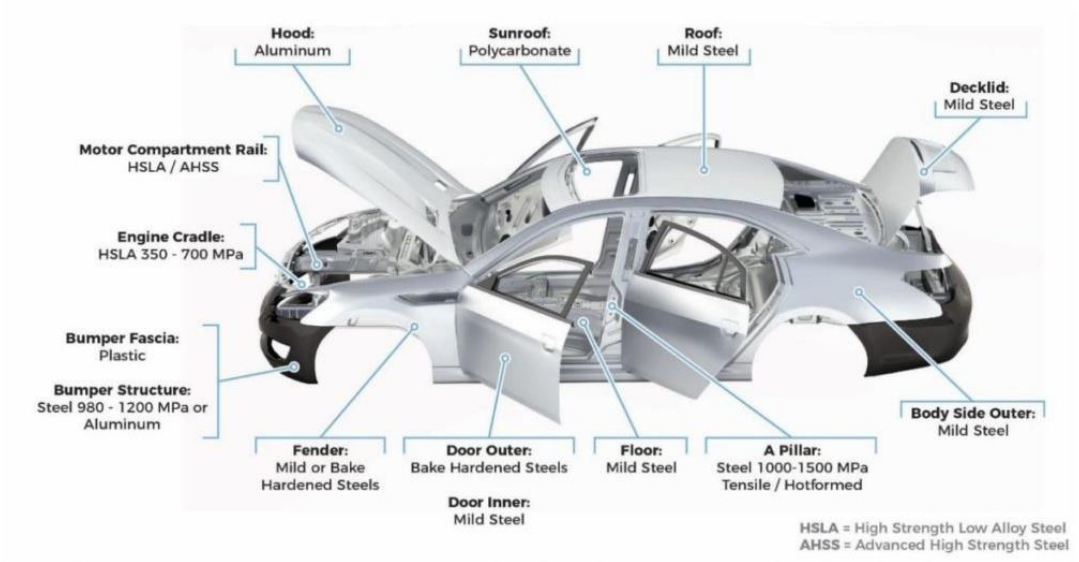

Figure 2.12. Material used for vehicular structural components [46].

2.4.1.2. Construction and Pipelines

Low carbon steel is extensively used in construction as main elements, jointing components, and reinforcements for concrete elements [4]. Various structures are created with low carbon steel, such as transmission towers, rail tracks and industrial buildings. Due to it is ability to be rolled, angles and sections are created with low carbon steel, in addition to sheets and bars [47].

2.4.1.3. Tools and Cookware

The functional and crucial components of hand tools that are used in manufacturing and construction are made from low carbon steel. The ability to obtain the best performance at lower thicknesses made low carbon steel the prime choice for designers of the tools. Subsequently, the weight of the tool is reduced with the use of less steel material. Low carbon steel is highly conductive for electricity and heat. Thus, isolation components, such as wood, plastic, and rubber, are used to substitute this disadvantage. However, the poor corrosion resistance of mild steels remains an issue, which requires durable coating [48].

2.4.2. Metallurgical Properties of Steel Alloys

There are various elements that are used to create steal alloys in order to improvement different performance criteria, such as corrosion resistance and thermal resistance. The ratio of the alloying elements does not exceed 5% wt.; however, their impact on the alloy strength or hardness. Alloyants are also added in higher percentages reaching to 20% wt. to enhance performance criteria related to thermal stability and corrosion [49]. Table 2.7 shows the different alloyants added to steel and the enhanced properties through their inclusion in the composition of the alloy.

Table 2.7. Elements added to steel alloys and the improved performance [49].

Element	% wt.	Improvement
Al	0.95 – 1.30	Utilized in nitriding steels
Bi	-	Machinability
B	0.001 – 0.003	Hardenability
Cr	0.5 – 2.0	Hardenability
	4 - 18	Resistance to corrosion
Cu	0.1 – 0.4	Resistance to corrosion
Pb	-	Machinability
Mn	.25 – 0.40	Combined with sulfur to prevent brittleness
	> 1	Hardenability increase
Mo	0.2 – 0.5	Grain growth inhibition
Ni	2 – 5	Toughness increase
	12 - 20	Resistance to corrosion
Si	0.2 – 0.7	Hardenability and strength increase
	2	Used in spring steel to increase yield strength
	Higher	Magnetic properties increase
S	0.08 – 0.15	Machinability improvement
Ti	-	Used in Cr steel to reduce martensitic hardness
W	-	Hardness increase with high temperatures
V	0.15	Maintaining ductility with an increase in strength and promoting fine grain structure

In steel composition, carbon has the most influence on the mechanical properties of the alloy, where low carbon steel has 0.1% wt. to 0.28% wt. carbon, a medium carbon steel has 0.3% wt. to 0.7% wt. carbon, and high carbon steel exceeds 0.7% wt. carbon [50]. Manganese is one of the most added elements to steel, which is used to avoid the development of iron sulfide leading to hot shortness defections [51], enhance mechanical properties [52], and improve hardenability to use of less brutal quenching to reach martensite [53]. If Manganese is added between 0.6% wt. and 0.8% wt. acicular ferrite is formed, which improves the tensile strength of steel. Acicular ferrite, also known as Widmanstatten structure, is ferrite-layer-like thin intergranular structure, which takes the shape of needles that follow different orientations, as shown in Figure 2.13. Toughness is increased with the addition of 0.6% wt. to 1.8% wt. of manganese, as well as the presence of acicular ferrite [50]. The yield strength increase is associated with the increase in acicular ferrite's dislocation density and fine grain. Thermal inputs through the welding process, especially above 20 kJ/cm contributes into the disappearance of acicular ferrite [54]. Proeutectoid ferrite, shown in Figure 2.13, is mixed with pearlite, which is a mixture of ferrite and Fe_3C, if the carbon content is less than 0.55% wt., while crystallographic networks appear enveloping the grains of pearlite if the carbon content is increased up to 0.85% wt. [50].

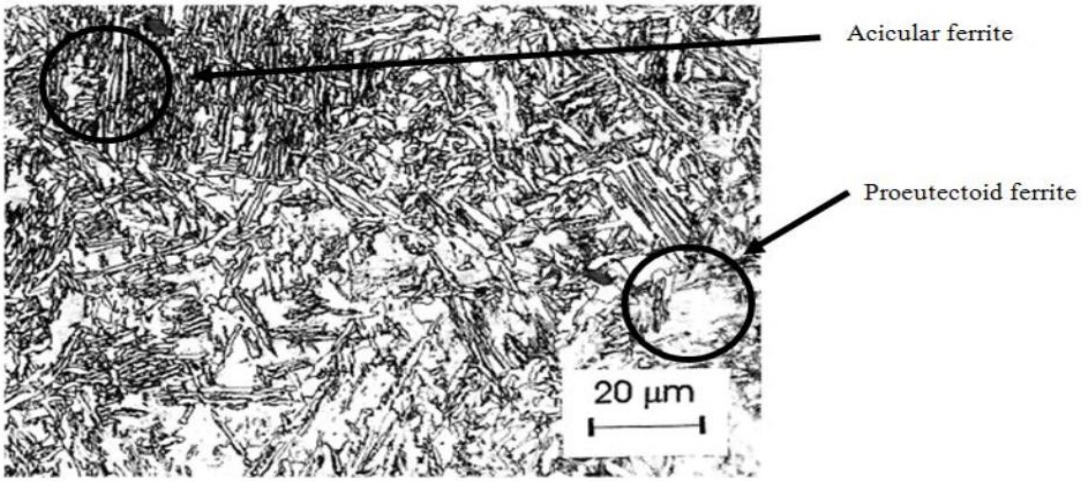

Figure 2.13. Microstructure imaging showing acicular and proeutectoid ferrites [55].

In deoxidized steels, silicon is used as an energetic deoxidizer, which removes the excess oxygen that dissolves in molten steel and develops blowholes during its solidification through reacting with the oxygen to form SiO_2 [56], as shown by the below equation:

$$Si + O_2 \rightarrow SiO_2$$

Figure 2.14 illustrates the equilibrium created between the oxygen and silicon contents in steel. Aluminum is used for the same purpose through forming Al_2O_3, as per the following equation:

$$4\ Al + 3\ O_2 \rightarrow 2\ Al_2O_3$$

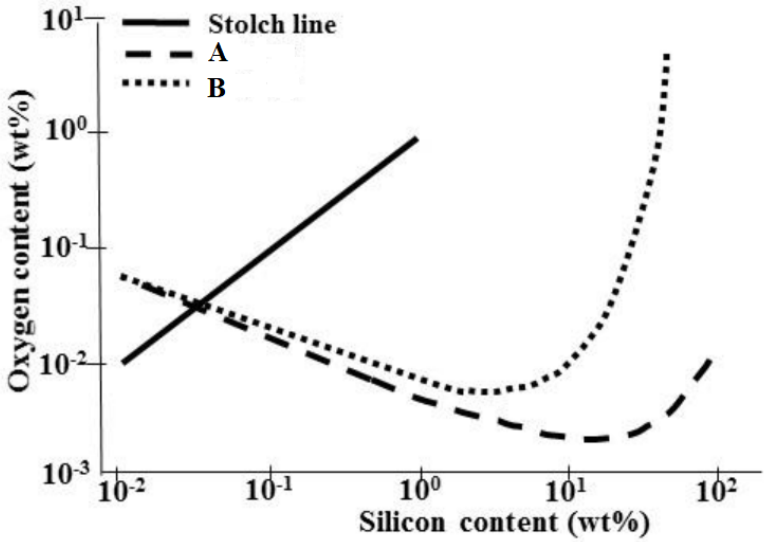

Figure 2.14. Equilibrium between oxygen and silicon contents in steel with comparison between A [54] and B [55].

The replacement of the base metal is avoided through retaining higher amount of oxygen by low concentrations of silicon. A comparison between silicon and other deoxidization elements, including aluminum, calcium, and manganese, showed that silicon had the highest ability to reduce the amount of oxygen [56].

Nonetheless, the use of other deoxidization elements like aluminum has other benefits by hindering grain growth and solidifying the steel leading to grain size refinement [57]. Additionally, the nitrogen content is improved in the steel through the addition of aluminum [58]. Moreover, the grains of steel are recrystallized, as shown in Figure 2.15, especially during steel annealing, with the presence of aluminum nitride, which enhances the mechanical properties of the steel through eliminating internal stresses, increasing ductility, and reducing hardness. Figure 2.16 show the relationship between temperature and recrystallization during annealing time.

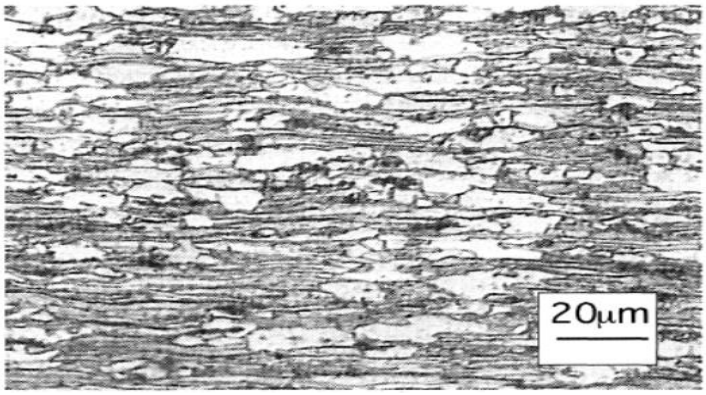

Figure 2.15. Partial recrystallized steel after 17 hours of annealing [57].

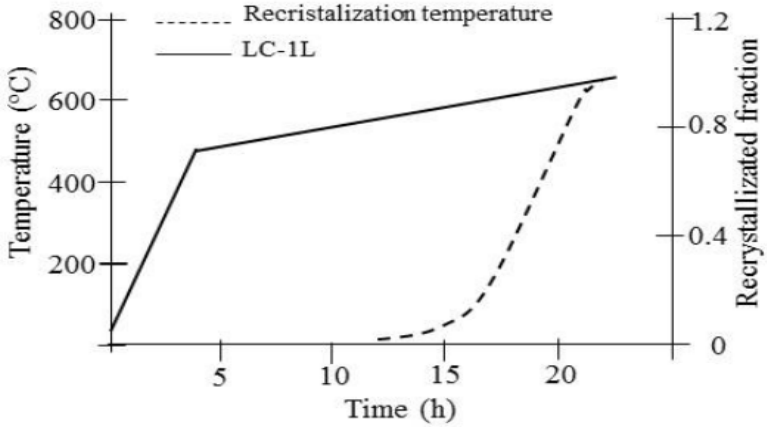

Figure 2.16. Impact of temperature on steel crystallization [57].

The ferrite phase is hardened, and yield strength is increased in steel through the rapid formation nitrides with iron through the addition of nitrogen [59]. At high

temperatures, the atmospheric nitrogen at the surface of the steel is interstitially diffused into steel through nitrogen infusion. Iron nitride is apparent in treated steel samples through its platelet precipitates, as shown in Figure 2.17. The increase in nitrogen concentration leads to the increase in surface hardness from 7.5 GPa to 14.4 GPa with a linear relationship, after exposing steel to nitrogen for 36 hours [59].

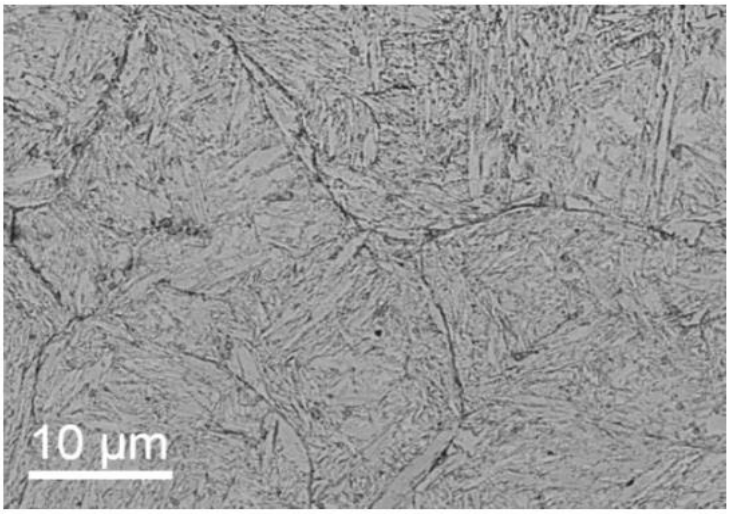

Figure 2.17. Platelets of iron nitride precipitates on steel surface through SEM [59].

The addition of 0.02% wt of niobium can increase the modulus of elasticity of steel between 68 MPa and 107 MPa by forming niobium carbides at high temperatures and its precipitation in the austenitic phase γ, which also increases strength and resilience properties [60]. Carbides, V_4C_3 type, are also formed through the addition of vanadium through its affinity to carbon or nitrogen, similar to niobium and chromium. The martensitic or austenitic phases are dislocated, and precipitates of small globular carbides are formed at grain boundaries with the addition of vanadium [61], as shown in Figure 2.18. The carbides formed by vanadium increase the strength and hardness of steel [62].

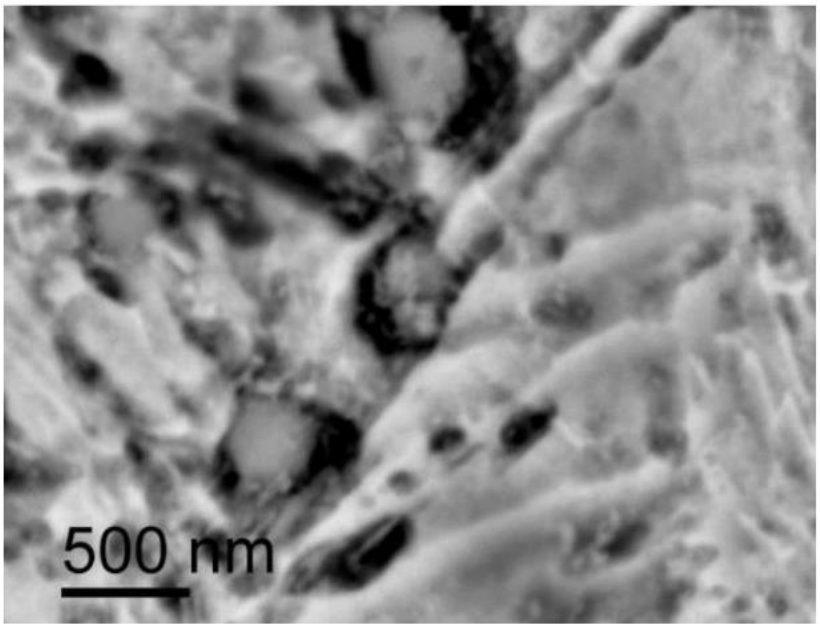

Figure 2.18. Precipitates of globular vanadium carbide at nanosized scale (dark zones) [59].

The machinability of steel is enhanced through the addition of phosphorus and Sulphur [63]. Cold-forming processes and drawability in high-strength steel is enhanced by adding phosphorus, while machining performance is enhanced through the addition of Sulphur. For instance, the increase of tool travel by 33% between 1018 steel and 1117 steel is only achieved due to Sulphur content [64]. Table 2.8 provides a summary of all the discussed elements and their implications on steel microstructure and properties.

Table 2.8. Impact of alloyants on the microstructure and properties of steel [64].

Alloyant	Typically added amount	Microstructure impact	Properties impact
N	0.012 – 0.025	Precipitates of iron nitrides	Hardness increase
Nb	0.05 – 0.08	Niobium carbide	Strength, modulus of elasticity and resilience increase
P	0.025 – 0.035	Precipitates of iron phosphate	Enhanced machinability
S	0.025 – 0.035	Precipitates of iron sulfide	Enhanced machinability
V	0.08 – 0.14	Precipitates of vanadium carbides	Hardness increase

2.5. EEFECTS OF ARC WELDING ON STEEL MATERIAL PROPERTIES

Welding imposes several changes on the metal through the changes in temperature and electrical current that is used for the process. It is argued that changes in the mechanical and microstructure properties are imposed on specimens through arc welding [65]. Therefore, this part of the study reviews a few studies to understand these changes in low carbon steel.

Bodude and Momohjimoh [66] experimented with two welding types: oxy-acetylene and shielded arc, where the welding processes were carried out with different voltages (100 and 120 V) and different currents (100, 120, and 150 A), as well as the heat that increases with the increase of these parameters. The findings show that hardness and tensile strength decreased with the increase in voltage and current, while the impact strength increased. The cooling rate of the welded area contributed significantly into the microstructure of the metal with variations in the ferrite and pearlite with the different welding conditions of the low carbon steel.

Boumerzoug, et al. [67] investigated the effects of arc welding on low carbon steel used in gas storage cylinders. The microstructure of the original metal showed ferrite regions as a vast majority within the structure, with limited pearlite at the corners and edges of grain boundaries. The grain size was mainly at the 10 μm average. Segregations at the pearlite bands were observed due to the presence of Mg, Cr and Mo. Following the arc welding process, the ferrite grains were observed to elongate with larger effect when approaching the fusion line. The orientation of the affected ferrite grains was along the heat flow.

Husaini, et al. [68] tested the welding connection of a ow carbon steel to understand the changes in microstructure and mechanical properties. Shielded metal arc welding was used in the experiment, where E7016 with 2-mm and 6-mm diameter was used an electrode. The maximum impact toughness values were recorded as 251 j/mm^2 and 119 j/mm^2 for the welded metal and the heat affect area, respectively. Hardness values increased from the base metal to the welded metal from 67.1 HR_B to 87.6 HR_B, while the increase was less at the heat affected zone to 73.9 HR_B. The

microstructure study showed changes in the ferrite and pearlite formations that increased towards the heat affected zone.

Sumardiyanto and Susilowati [69] experimented arc welding effects on low carbon steel using different electrode types and electric currents. Significant differences were found in mechanical properties with the changes of the welding conditions, especially in tensile strength, hardness, and impact. While hardness and impact decreased after arc welding, the results on tensile strength varied greatly with the changes in electrodes and currents. Generally, the tensile strength decreased with the increase of electrical current, while the highest value for tensile strength was found with the use of E7016 as an electrode.

2.6. MECHANISM OF SHOT PEENING

Shot peeing is performed on various types of materials through bombarding their surface with small spherical bodies, and it is a type of cold working processes [12]. The spherical bodies act as a tiny peening hammer when they strike the surface, which cause simples and indentations. As a result of the process, fibers below the surface attempt restoring the surface to the original shape, which cause compression stresses at each point-of-work. A more complex residual stresses are formed with the overlap of dimples at the same or close points. At compressively stressed zones, it is unlikely for cracks to develop or disseminate. Through simulating the compressive stresses with shot peeing, failures caused by stress corrosion and fatigue that originate at the surface of the material are avoided [70]. The local compressive strength induced by shot peeing is equal to at least half of the material's yield strength, and hardness increases with the process. Several failures are treated through shot peeing, including fretting, cavitation erosion, galling, stress by corrosion cracking, fatigue, cracking simulated by hydrogen [71].

The stresses that are maintained within the material without the application of external loads, after manufacturing processes are finalized, are called residual stresses, which vary into compressive and tensile forces. The compressive stresses created by shot peening are the most influential in obtaining the benefits of the

treatment. Figure 2.19 shows the changes of the profile of residual compressive stress that is resulting from shot peeing [72].

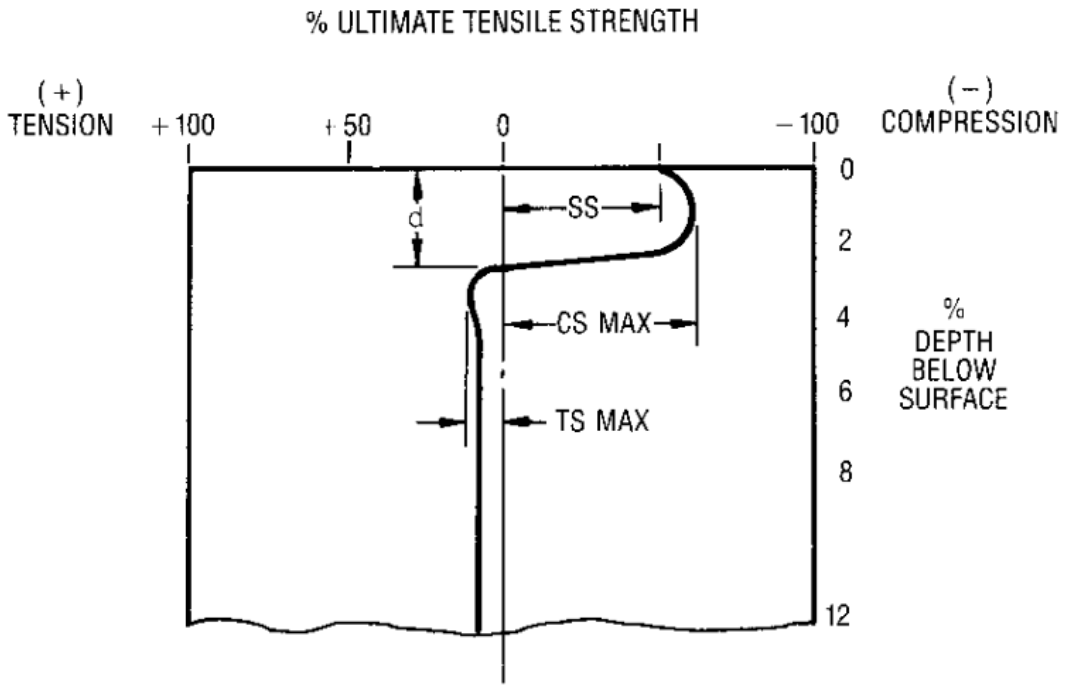

Figure 2.19. Changes in the profile of residual stress with shot peening [72].

From the above figure [72]:

- Ts_{max} is the maximum value of the simulated tensile stress. An equilibrium is created through an offset tensile stress at the core that balances the compressive stress at the surface, while its value should not be too high to the extent of creating internal failures.
- Cs_{max} is the shot peeing maximum compressive strength as it is the highest at the surface.
- SS is the stress measured at the surface (surface stress).
- d is the cross point of the compressive stress towards the tensile stress reaction at the neutral axis.

The magnitude of the induced residual stress is another way to describe Cs_{max}, where its variation does not highly influence magnitude as long as the used shots has

hardness values that are equal or more than the hardness value of the shot peened material. As shown in Figure 2.20, the magnitude of Cs_{max} is at least 1.5 times the yield strength of the material and it is a function of the shot peened material [73].

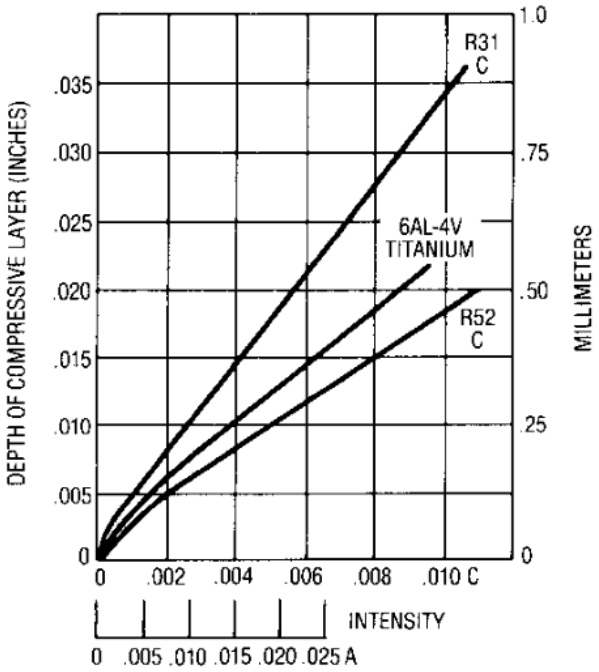

Figure 2.20. Relationship between tensile strength of steel and residual stressed induced by shot peeing [73].

The changes in the shot peeing parameters determines the depth of the compressive layer. The above Figure 2.24 illustrates the relationship between the intensity of shot peeing that changes with the type of material used and the depth of the compressive layer [73].

In specimens with smooth surfaces, shot peeing on the lower and upper surfaces exerts no external load, as shown in Figure 2.21. The stress distribution curve illustrates the equilibrium created between the tensile and compressive stressed, in the case of no external loads applied, which means that the stress distribution areas below and above the surface must be equal with the total moment equal to zero for the areas [74].

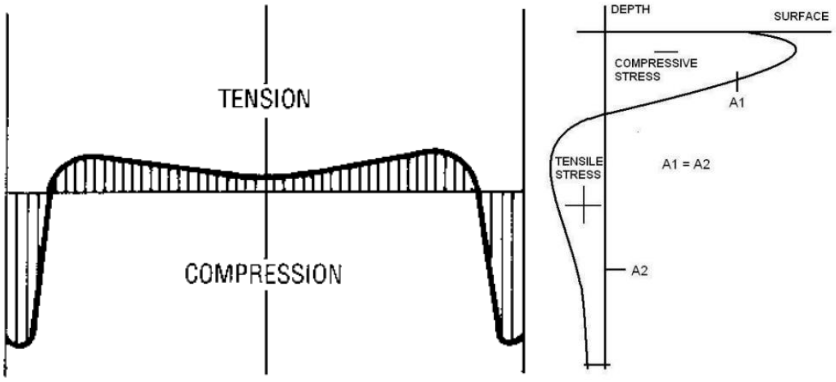

Figure 2.21. Distribution of residual stress after shot peening [74].

Figure 2.22 illustrates the bending moment application for the stresses of Figure 2.25 (left graph), where at any given depth, the sum of the applied load at the depth and the residual stress produces the value of the resultant stress. The dashed line represents the bending load, while the solid line represents the resultant curve of the stress distribution. The compressive strength induced by shot peening reduces to a great extent the stress at the peened surface, which prevents surface cracks from initiating and propagating [73].

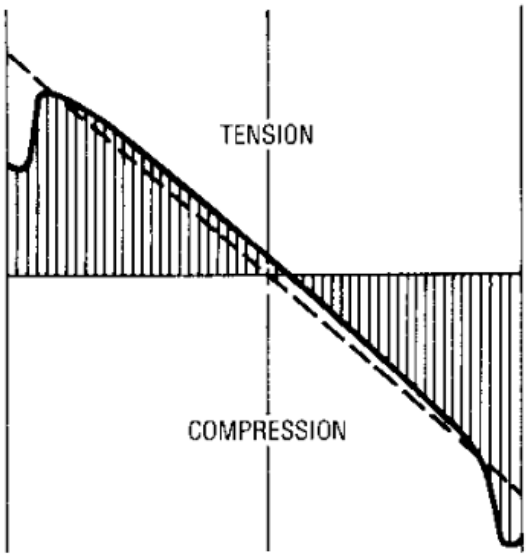

Figure 2.22. Residual and applied shot peening stresses at superposition [73].

In notched specimens, effective stress is increased and highly concentrated at the surface, as illustrated through the distribution of stress with a Kt = 2 bending load in Figure 2.23 [73].

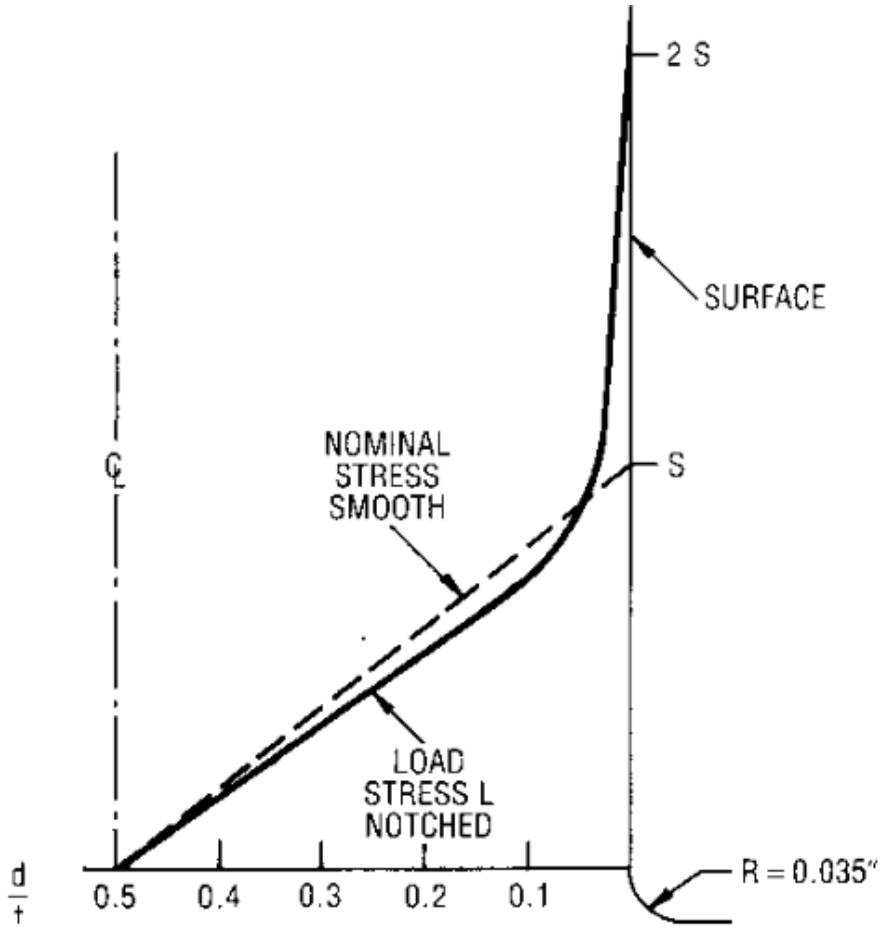

Figure 2.23. Bending stress distribution in notched specimens [73].

The profile of stress and load for a notched specimen after it was shot peened is shown in Figure 2.24. Fifty percent of the effect of the stress at the surface caused by the bending stress is reduced as a result of treatment with shot peening [73].

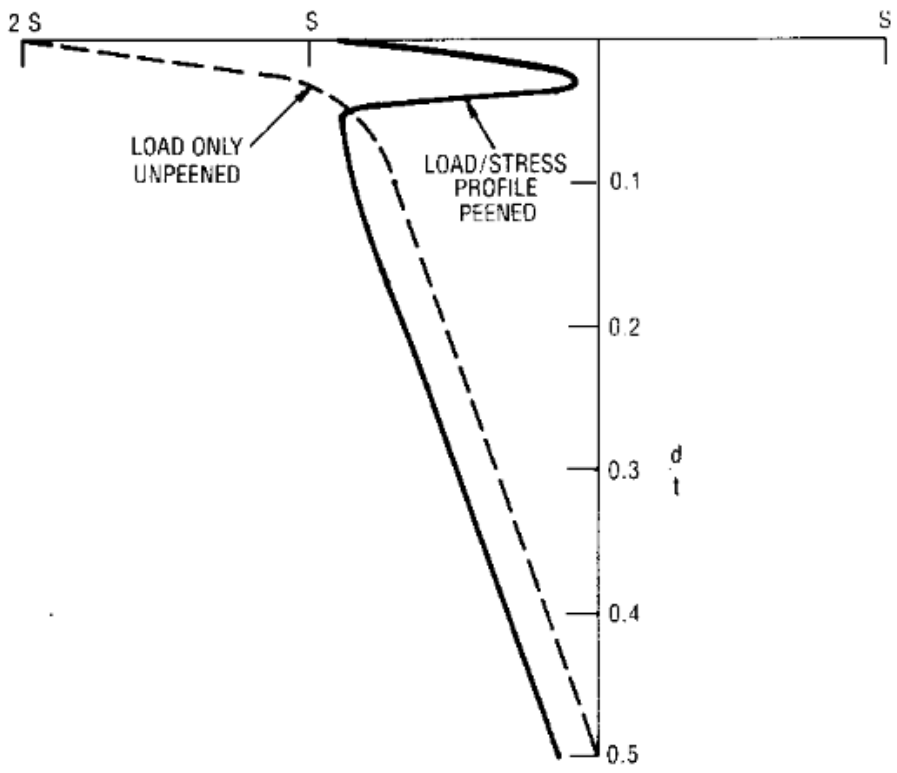

Figure 2.24. Distribution of stress and load for bending a shot peened specimen [73].

CHAPTER 3

METHODOLOGY AND EXPERIMENT

3.1. MATERIAL

The alloy used in this experiment is ST37-2 (a typical metal content percentages are shown in Table 3.1). The alloy has a maximum carbon content of 0.2% and nitrogen content of 0.011%. The tensile strength of the alloy ranges between 360 and 460 MPa, yields at 235 MPa with a minimum elongation of 25% [75].

Table 3.1. Chemical composition of ST37-2 (%) [76].

Fe	Mn	Si	Al	Cr	Cu	Ni	P	S
98.7012	1.0916	0.0641	0.0408	0.0285	0.0253	0.0235	0.0158	0.0091

3.2. SAMPLE PREPARATION

After cleaning the steel plates, samples were initially prepared with specific dimensions. Each two plates were welded with an arc welding device to form a single plate, as shown in Figure 3.1. The welding slag was removed with an electric grinding machine. Using a plasma cut, two specimens of welded plates were cut into several samples, according to the schematic shown in Figure 3.2. A group of specimens were prepared for tensile testing, while another group was prepared for fatigue testing. The sample dimensions followed the ASTM specifications of the testing specimens. Figure 3.3 shows the specimens for the tensile testing.

Figure 3.1. Arc welding of steel plates.

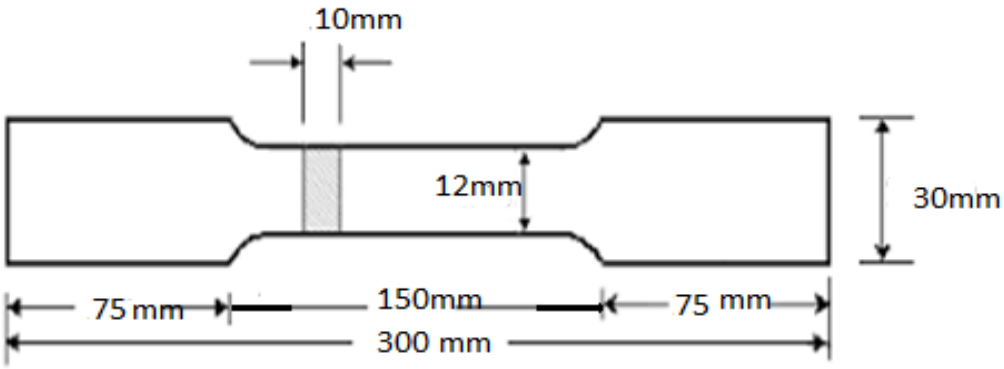

Figure 3.2. Schematic of tested specimens.

Figure 3.3. Samples for tensile testing (top) and fatigue testing (bottom).

Four out of the six specimens were shot peened with two Almen intensities, A12-14 (CSP) and A28-30 (SSP). The shot peening conditions are shown in Table 3.2.

Table 3.2. Conditions of shot peening for CSP (Conventional) and SSP (Severe).

Almen Intensity	Shot Size	Coverage	Duration (sec)	Air Pressure (psi)	Arc Height (mm)
A12-14 (CSP)	S230	200%	10	30	0.13
A28-30 (SSP)	S230	200%	15	60	0.29

The process of shot peening involves striking the samples with tiny particles with a specific pressure that act as a hammer on a small area of the surface in order to create indentations or dimples [77].

The processes energize the particles with kinetic energy that is absorbed by the metal surface [78]. As a reaction, the metal surface absorbs the energy and attempts to restore its original condition [79]. The main target of using shot peening is to increase the hardness and fatigue resistance of the samples, while reducing tension [80]. Figure 3.4 and Figure 3.5 show the surfaces of the metals using the two types of shot peening. The top picture shows shot peening with A12-14 Almen, while the bottom picture shows shot peening with A28-30 Almen.

Figure 3.4. Surface of ST37-2 after shot peening; A12-14.

Figure 3.5. Surface of ST37-2 after shot peening; A28-30.

3.3. MICROSTRUCTURAL CHARACTERIZATION AND PHASE ANALYSIS

Rigaku ULTRA IV Diffractometer is used for phase identification in the XRD analysis. The settings of the diffractometer were set, as follows:

- 20 mA current
- Cu-Kα-X-ray radiation below 40 kV acceleration voltage
- 3 degrees per minutes as the measurement scan speed
- Scan range is 20° to 90°

For identification of the material's Xray diffraction pattern, the ICDD database was used.

Three microstructural characterization tested were performed: Field Emission Scanning Electron Microscopy (FESEM) with Carl Zeiss ULTRA PLUS FESEM, chemical composition assessment with Energy Dispersive Spectroscopy (EDS) with Carl Zeiss EVO 18, and optical microscope image analysis using Nikon Eclipse MA200 inverted optical microscope powered with Clemex Vision Lite software.

3.4. ROUGHNESS TEST

Surface roughness for the specimens was measured with MITUTOYO Surftest 211 (Figure 3.6) to obtain the Ra, Rq and Rz values. The device was put against each sample in different and readings were obtained.

Figure 3.6. MITUTOYO Surftest 211.

3.5. TENSILE TEST

Zwich/Roell Z600 Universal Test Machine (Figure 3.7) was used to carry out the tensile test. Specimens were tested according to ASTM D-638, ASTM D-3039 and ASTM C-297 standards.

Figure 3.7. Zwich/Roell Z600 universal test machine.

3.6. HARDNESS TEST

Q10 A+ QNESS microhardness testing machine (Figure 3.8) was used to perform Vickers microhardness test with a 1000-gram load and 15 seconds holding time. The average measurement at three different points was calculated to produce the hardness value at one indentation per point.

Figure 3.8. Q10 A+ QNESS microhardness testing machine.

CHAPTER 4

RESULTS AND DISCUSSION

4.1. ROUGHNESS TEST

Three samples were tested for surface roughness for untreated, type A12-14 shot peening and type A28-30 shot peening. The average roughness (Ra), root mean square roughness (Rq) and average maximum height of roughness profile (Rz) were obtained, as shown in Table 4.1. The outputs of the test are plotted for the untreated sample, CSP sample, and SSP sample in Figure 4.1, Figure 4.2, and Figure 4.3. respectively. The results show a significant increase in roughness between the untreated metal and the CSP cases, while more increase in roughness can be observed in SSP cases. These results are expected and were shown similarly in the literature. Omari, et al. [81] increased hardness and roughness for engine bladed with shot peening. Liu, et al. [82] showed that the increase in shot peening severity increased surface roughness in ZK60 alloy.

Table 4.1. Surface roughness values.

Material	Almen intensity	Ra	Rq	Rz
ST37-2 STEEL	A12-14 (CSP)	6.568	8.174	32.267
ST37-2 STEEL	A28-30 (SSP)	7.466	8.907	34.432
ST37-2 STEEL	As received	0.198	0.253	1.432

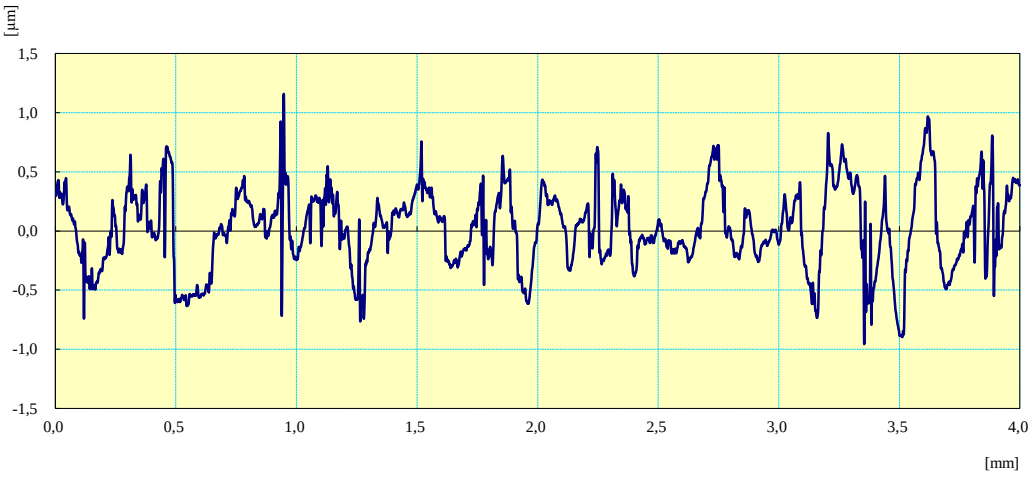

Figure 4.1. Roughness test profile for untreated sample.

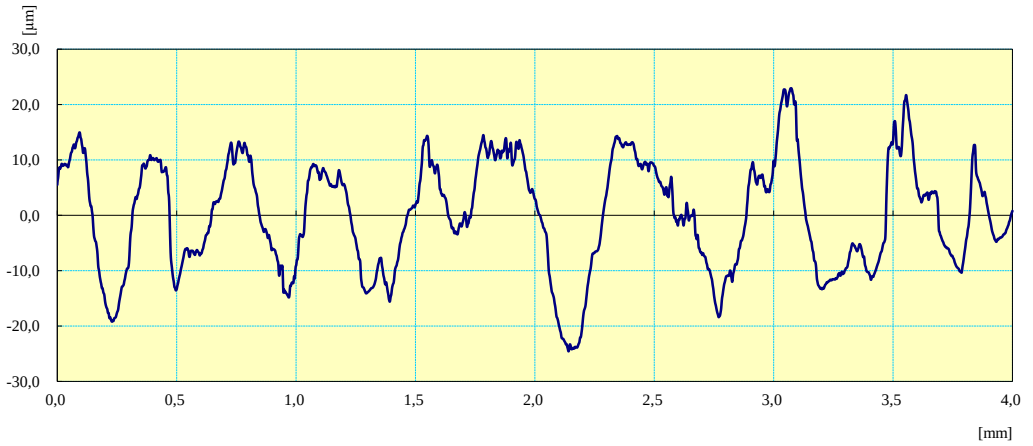

Figure 4.2. Roughness test profile for CSP sample (A12-14).

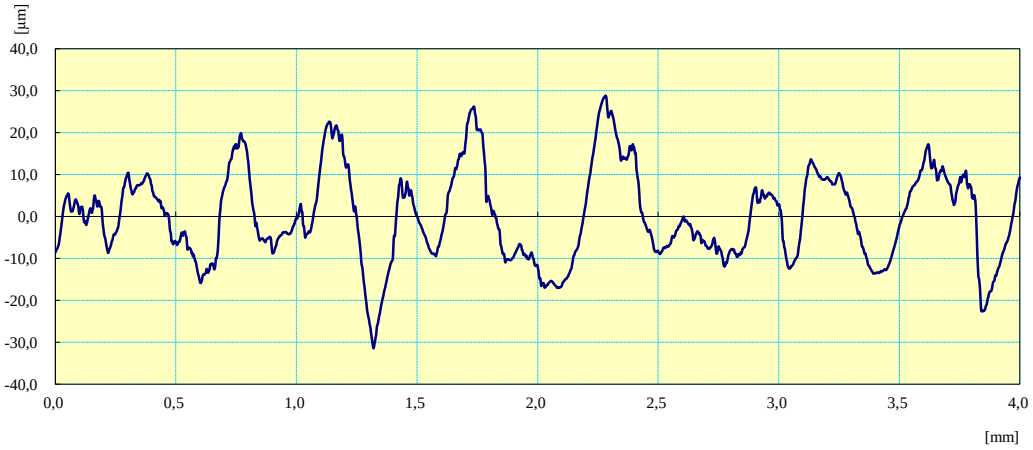

Figure 4.3. Roughness test profile for SSP (A28-30).

4.2. TENSILE TEST

The force required to break a specimen and its elongation are measured through a tensile strength test according to ASTM D-638, ASTM D-3039 and ASTM C-297 standards. The test outputs are shown in Table 4.2 below.

Table 4.2. Tensile strength test outputs.

Specimen designation		**Base II**	**Base Empty**	**A12-14-1**	**A12-14-2**	**A28-30-1**	**A28-30-2**
L_c	mm	80	80	80	80	80	80
m_E	GPa	189,4489	247,255	202,6775	197,705	184,482	196,6982
$R_{p0.2}$	MPa	359,9083	431,0844	352,4638	348,8153	356,9212	348,0758
R_m	MPa	482,4395	564,5672	478,1755	468,7683	472,2603	468,6472
F_m	kN	59,93345	58,73193	59,39657	58,70855	58,32038	58,98394
A_g	%	12,38113	10,35529	11,15856	9,73384	10,54683	10,47944
A_{80}	%	23,67727	13,33054	24,72023	18,2359	20,70432	23,22652
a_0	mm	12,3	10,3	10,14	10,1	10,04	10,15
b_0	mm	10,1	10,1	12,25	12,4	12,3	12,4
ds/dt_{Set}	MPa/s	30	30	30	30	30	30
ds/dt_{Actual}	MPa/s	83,26168	95,06685	83,01809	82,44185	83,06666	83,01711
$V_{Actual\ crossh.}$	mm/min	6,388361	6,130087	6,388163	6,401271	6,378935	6,409216
$V_{Set\ crossh.}$	mm/min	2,301789	1,934456	2,308472	2,329377	2,303789	2,316107
$k_{Test\ assembly}$	kN/mm	-89,5097	-65,3467	-89,7389	-91,245	-89,0492	-91,2068
S_0	mm²	124,23	104,03	124,215	125,24	123,492	125,86

As shown in Table 4.3, the first sample treated with type A28-30 shot peening retained the yield strength of 360 MPa, while the ultimate tensile strength enhanced

by less than 5%. Elongation for the first sample decreased by around 5%. The changes are considered insignificant for the first sample. However, the second sample treated with type A28-30 shot peening showed more significant results as yield strength increased by 19.7%, ultimate tensile strength increased by 22.8% and elongation decreased by at least 46.8%.

Table 4.3. Results of tensile strength testing.

Material	Almen intensity	YS (MPa)	UTS (MPa)	Elongation (%)
St37-2 steel	A28-30	360	482	23.7
	A28-30	431	565	13.3
	A12-14	352	478	24.7
	A12-14	357	472	20.7
	As received	349	469	18.2
	As received	348	469	23.2

The results indicate an increased tensile strength accompanied with decreased ductility of the sample. Samples treated with shot peening type A12-14 and those that were not treated with shot peening showed insignificant changes in yield strength and ultimate tensile strength.

Figures 4.4, 4.5 and 4.6 show plots of the tensile test results for the six samples: untreated, CSP and SSP, respectively. Nonetheless, elongations have decreased at least between 1.2% to 27.2%, confirming the effect of shot peening on the ductility of the alloy. These results are based on standard range values of ST37-2. However, other studies showed yield strength and ultimate tensile strength values for the alloy of 235 MPa and 436.8 MPa, respectively, for untreated samples. Therefore, the results of the current study are considered all significant in comparison to such results [83].

The results also show that severe shot peening (SSP) with type A28-30 showed enhanced tensile strength in comparison with conventional shot peening (CSP), which confirms the results of the literature in this aspect [84]. Generally, shot peening showed enhanced strengths in comparison with samples that were untreated [81].

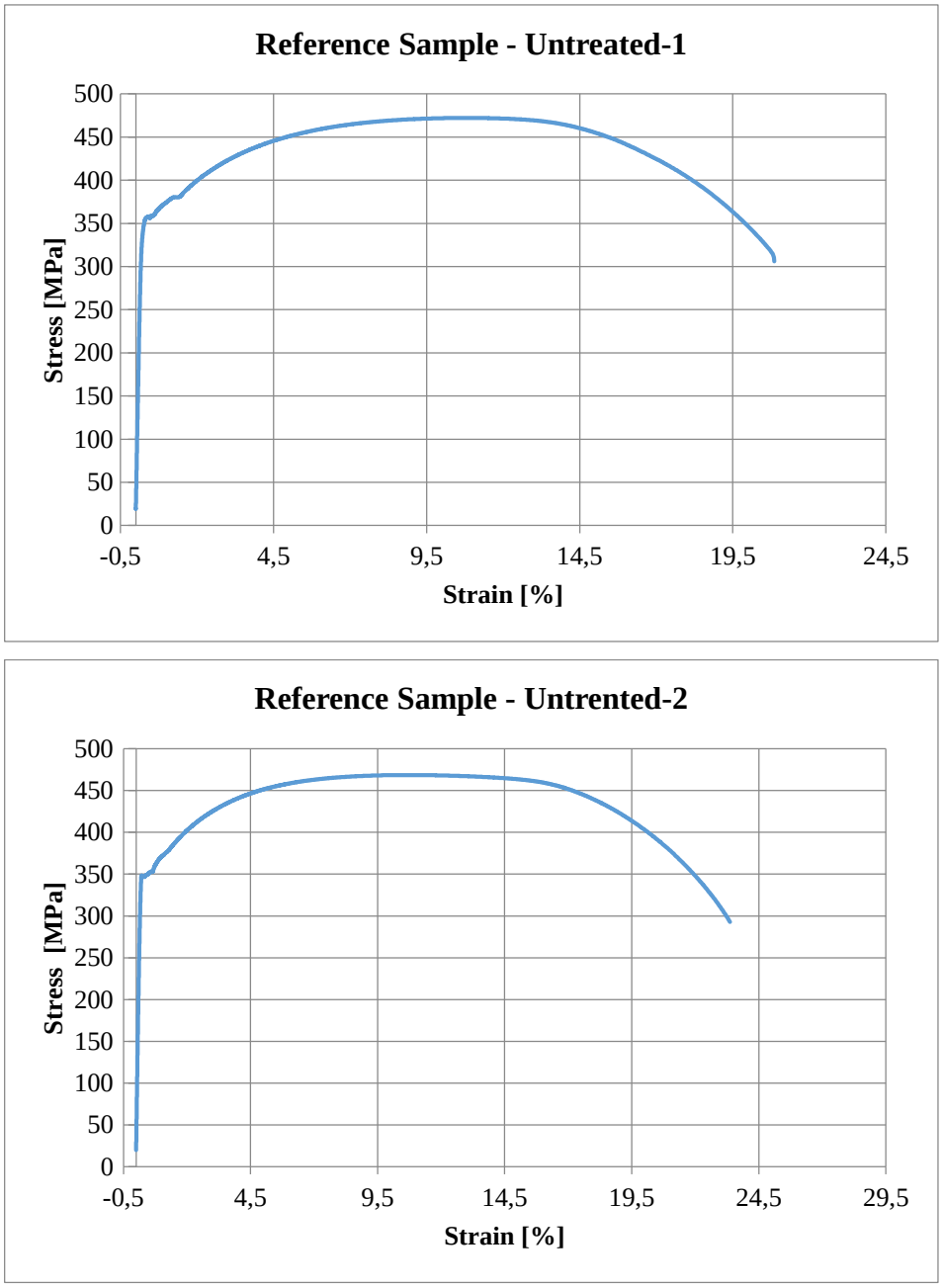

Figure 4.4. Tensile test plots for untreated samples.

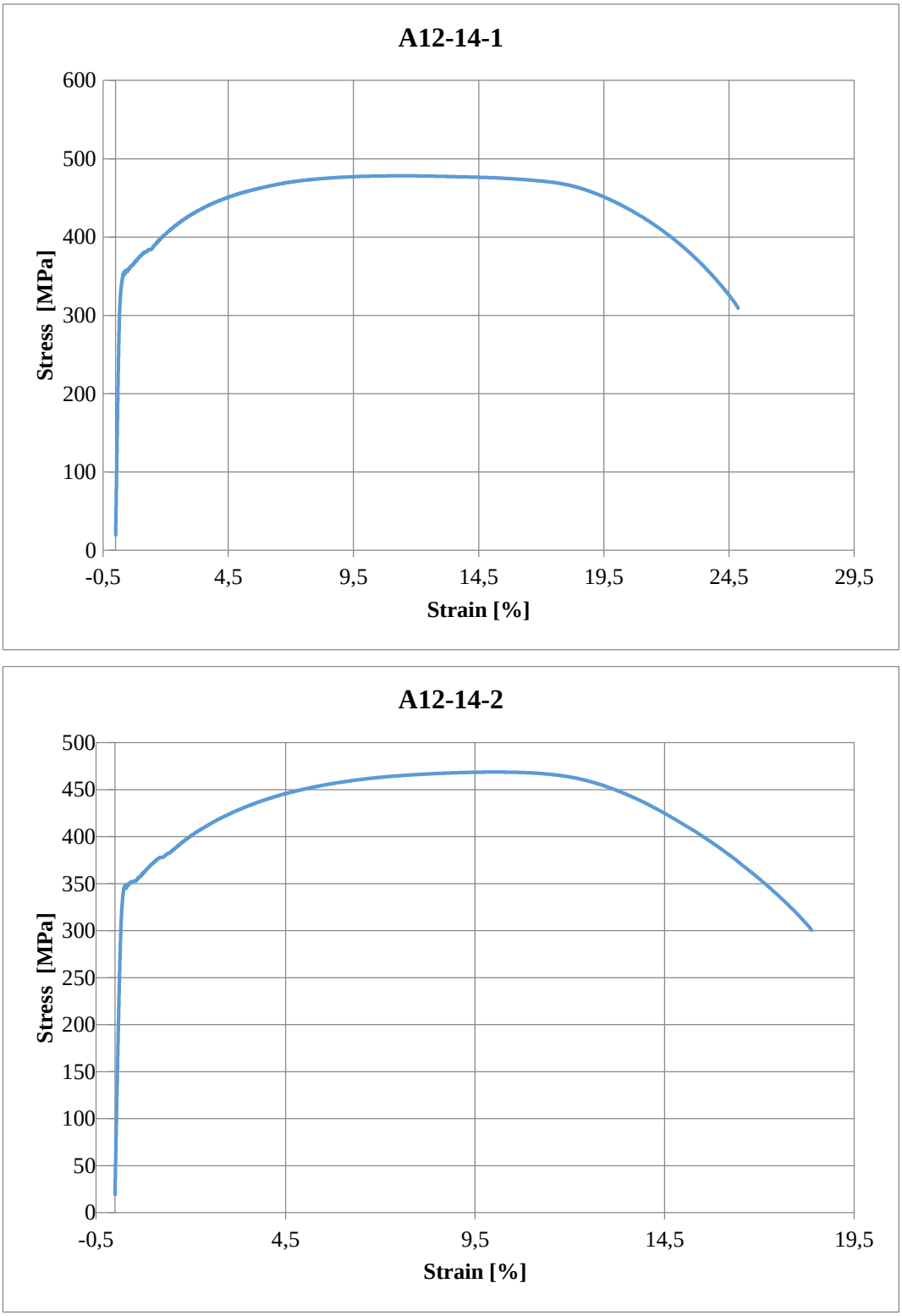

Figure 4.5. Tensile test plots for CSP samples.

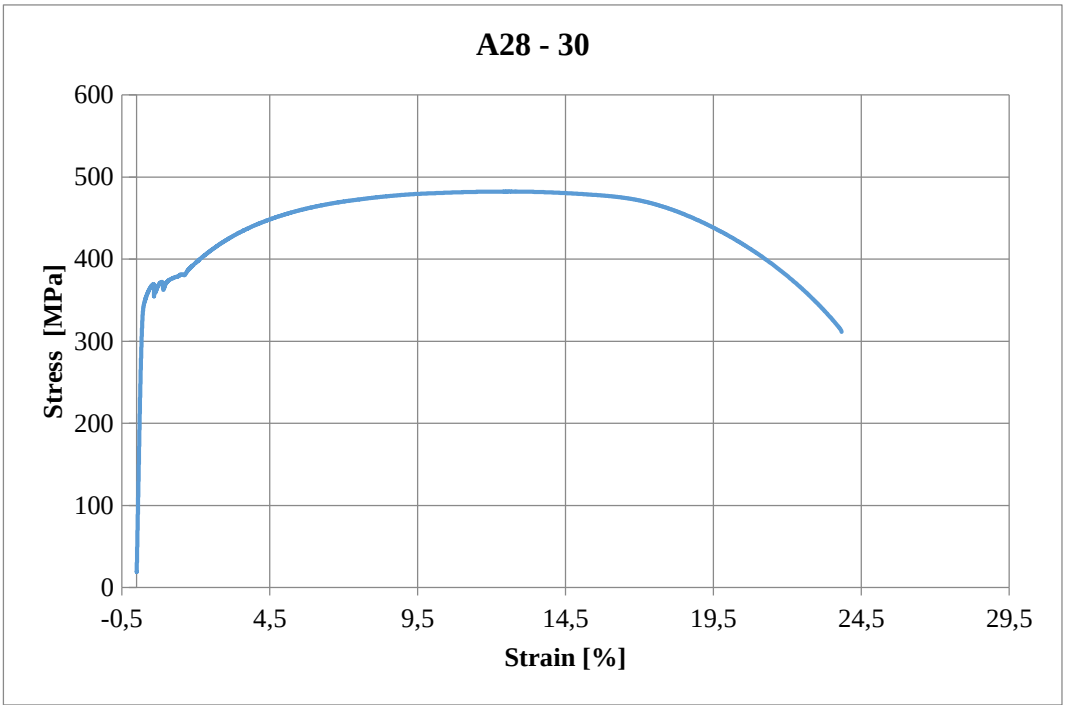

Figure 4.6. Tensile test plot for SSP sample.

4.3. MICROHARDNESS

Vickers microhardness test is conducted through applying a load of 1 kilogram for 15 seconds by a ball indicator. Values are measured through a calibrated optical microscope for the stress in MPa, as shown in Table 4.4 and Figure 4.7. As shown in results, shot peening increased microhardness from its original value of 150 for ST37-2 from 21.1% to 47.6% by average [85]. Another study showed that microhardness for low carbon steel has an average value of 92, which proves that the obtained hardness values in the current study are a huge enhancement [86].

Table 4.4. Vickers microhardness test values.

Almen intensity	Value (1)	Value (2)	Value (3)	Average
A28-30	222	224	218	221.33
A12-14	189	192	188	189.67
As received	183	181	181	181.67

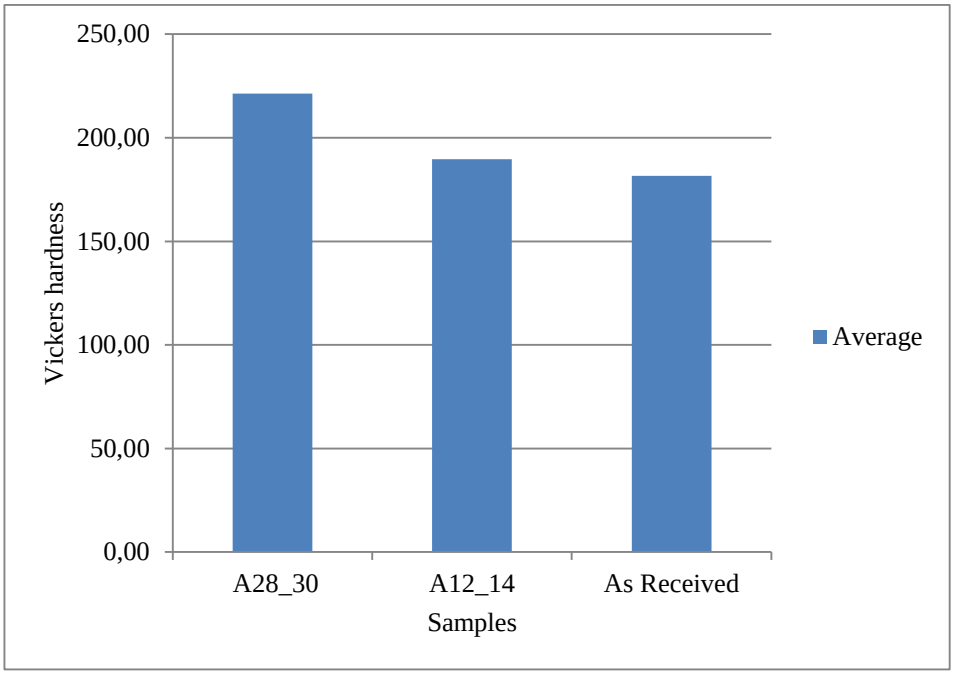

Figure 4.7. Vickers hardness values of the investigated alloys.

4.4. XRF ANALYSIS

X-ray fluorescence (XRF) is a microscopy method that is used to measure the concentration of metals in a specified area. The method depend on the interaction between the x-ray arrays with the matter through dislodging electrons from atoms and measuring the energy resulting to correlate it with a specific element [87]. As seen from the results of the XRF analysis in the current research (Table 4.5), the mass percentage of each metal component has been changed through shot peening, while the analysis depth ranged between 0.0009 to 0.0355 mm.

Table 4.5. XRF analysis for ST37-2.

Component	Result	Unit	EI line	Det. Limit	Intensity	w/o normal	Analyzing depth (mm)
Al	0.0408	Mass%	0.00204	Al-KA	0.3807	0.0418	0.0009
Si	0.0641	Mass%	0.00205	Si-KA	0.6215	0.0656	0.0013
P	0.0158	Mass%	0.00103	P-KA	0.4290	0.0161	0.0018
S	0.0091	Mass%	0.00072	S-KA	0.2240	0.0093	0.0025
Cr	0.0285	Mass%	000432	Cr-KA	0.6336	0.0292	0.0230
Mn	1.0916	Mass%	0.00870	Mn-KA	20.4876	1.1177	0.0265
Fe	98.7012	Mass%	0.02378	Fe-KA	2319.6146	101.0629	0.0355
Ni	0.0235	Mass%	0.00802	Ni-KA	0.2879	0.0241	0.0066
Cu	0.0253	Mass%	0.00556	Cu-KA	0.3890	0.0259	0.0104

4.5. XRD ANALYSIS

In order to identify crystalline material in the samples that were treated with shot peening, an x-ray powder diffraction (XRD) analysis is used. Figure 4.8 shows the peaks of three samples, which are identical in phase pattern and position, while differing in intensity. The matching patterns and positions are signs of error absence in positioning during the experiment. The slightly higher broadening at 64.85 and 82.27 degrees indicate minor nanocrystalline ceria. The three peaks shown in the figure show that changes in the micro-strains have occurred with shot peening and their intensities decreased with the increase of the severity of the deformation through shot peening in the metal.

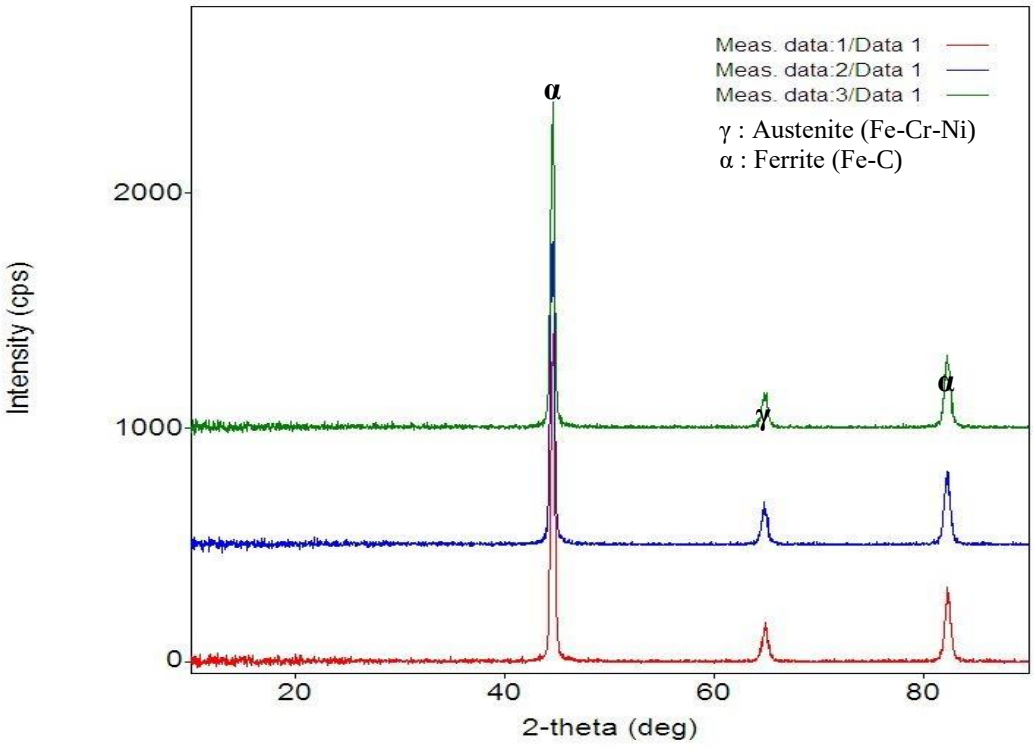

Figure 4.8. Diffractogram of XRD analysis.

4.6. OPTICAL MICROSCOPE

Two specimens were investigated using optical microscope to study the microstructure and mechanical changes of the shot peening treatment. Images are presented at 50 μm for comparison. Shot peening with CSP A12-14 Almen intensity,

Figure 4.9, affected a thin layer with minimum influence, while shot peening with SSP A28-30 Almen intensity, Figure 4.10, had a higher intensive influence with a thicker layer. In the SSP case, an intrinsic structure is observed. The ferrite and perlite phases are clear with SSP A28-30 [88]. Further images are provided in Figures 4.XX and 4.XXX for CSP and SSP shot peened samples, respectively.

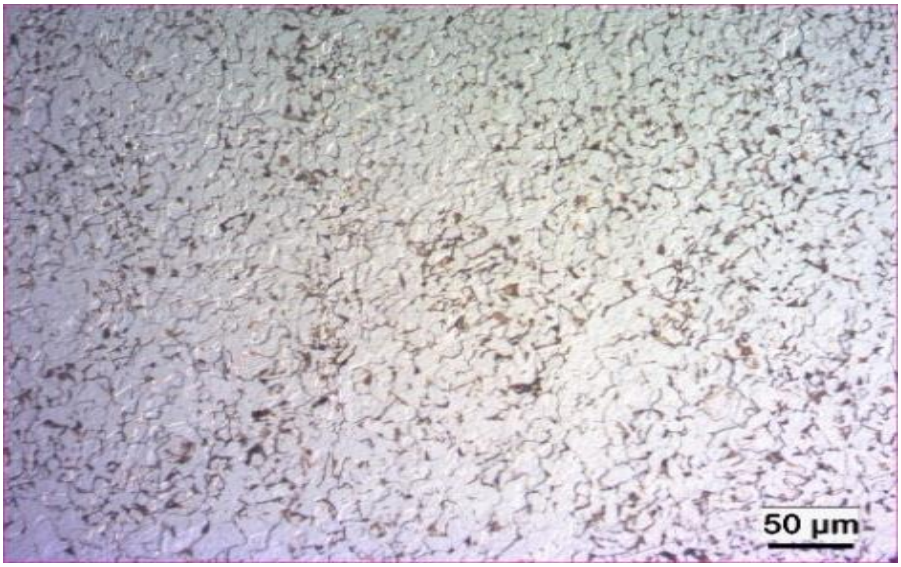

Figure 4.9. Optical microscope images for shot peened CSP A12-14 sample.

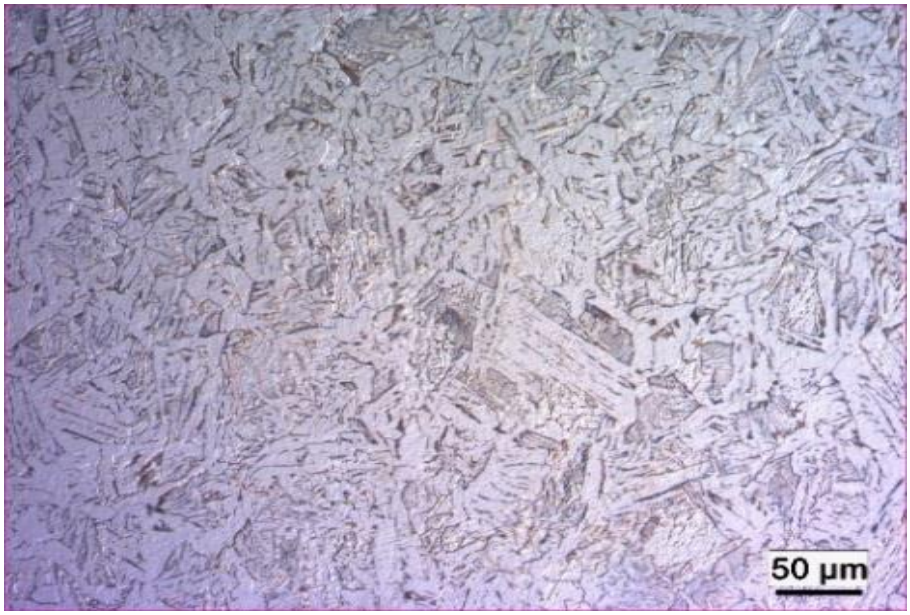

Figure 4.10. Optical microscope images for shot peened SSP A28-30 sample.

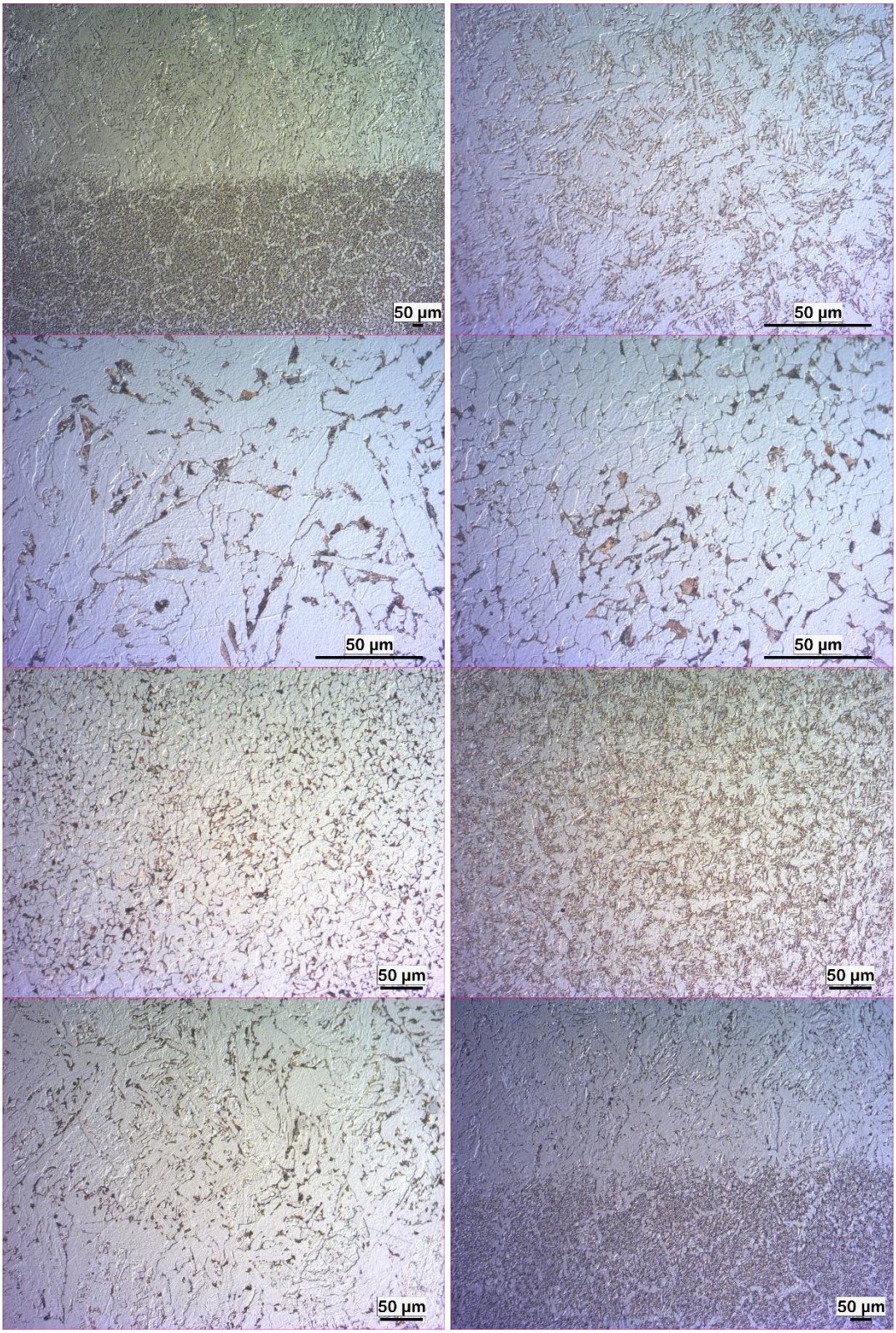

Figure 4.11. Additional optical microscopy for CSP samples.

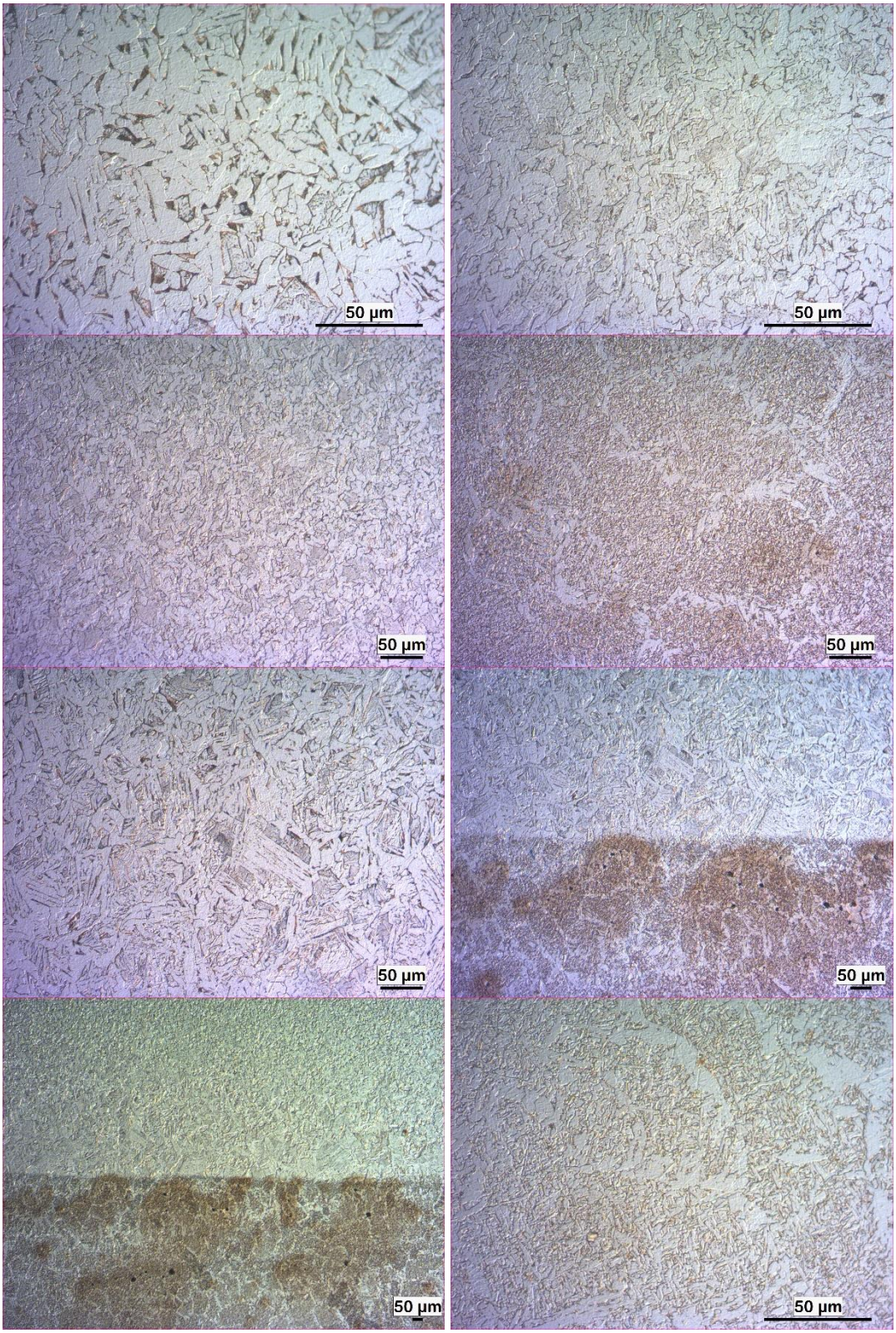

Figure 4.12. Additional optical microscopy for SSP samples.

4.7. SCANNING ELECTRON MICROSCOPY (SEM) OBSERVATIONS

The specimens treated with shot peening are tested with scanning electron microscopy. Both A12-18, Figure 4.13, and A28-30, Figure 4.14, Almen intensities yielded plastic deformations as illustrated. Disturbances are increased in the SSP case, while it created more intense bumps and pits. Layer thickness is increased by 24.4% with the SSP case in comparison with the CSP case. The homogeneity of the alloy does not seem to be affected in both samples by shot peening; however, the increase in hardness as confirmed by the hardness test is reflected by the formation of connected deformed structures [89].

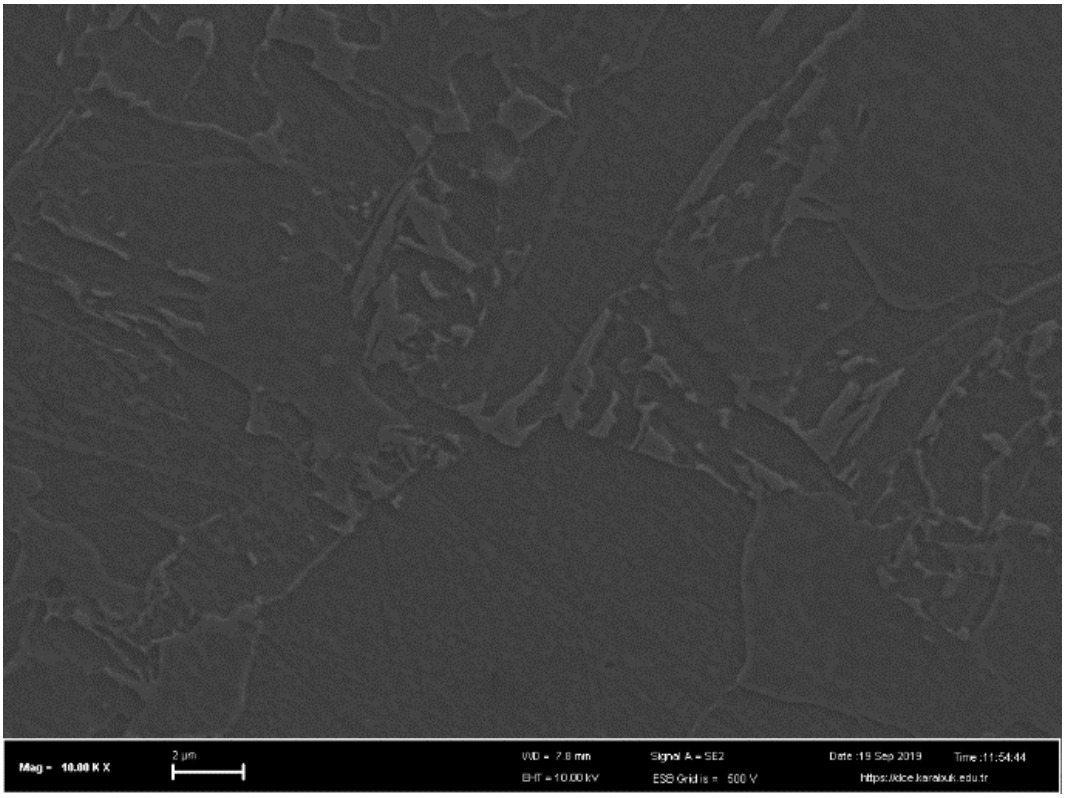

Figure 4.13. FESEM images of plastic deformed layer of shot peened specimen: CSP A12-14 (top-layer thickness = 7.8 μm).

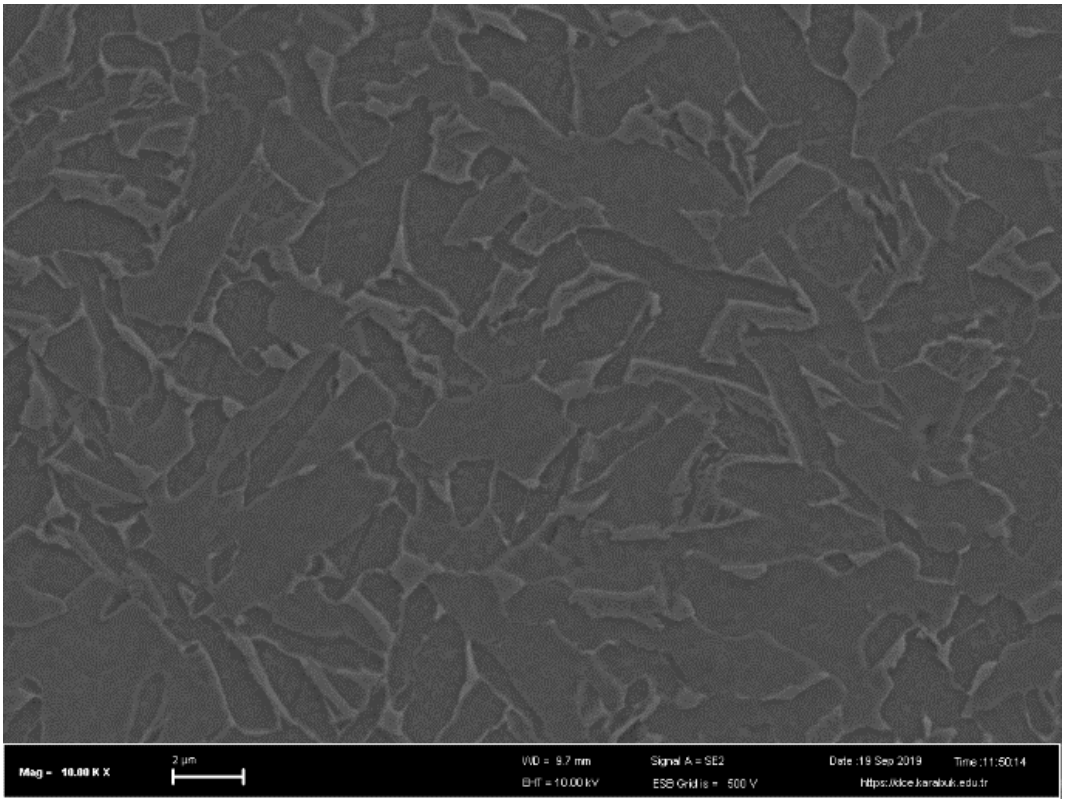

Figure 4.14. FESEM images of plastic deformed layer of shot peened specimen: SSP A28-30 (bottom-layer thickness = 9.7 µm).

CHAPTER 5

CONCLUSIONS

ST37-2is a low carbon mild steel that is mostly used as a structural metal due to several performance criteria it possesses. The alloy has excellent weldability and good ductility, which qualified it to be used in many applications, including shelters and water vessels, and can be shaped for several purposes as angles, strips, sheets, and plates. ST37-2 is a low carbon steel used for structural purposes, and it is also non-alloy in its standard form processed through hot rolling. It has a relative density of 7.85 kg/dm^3, according to volumetric mass calculations.

Surface treatment using cold techniques is widely used to enhance the mechanical properties of the metal alloys. Shot peening is one of these processes that has its impact on the surface roughness, residual stresses, microstructure and folding of the metal. The effects of plastic deformations resulting from welding or shot peening can be beneficial or have adverse effects on its strength and ductility. Severe plastic deformation (SPD) is formed in metals through processes, such as hydrostatic extrusion, which performs deformations in the metal at low temperatures, in comparison with other techniques. SPD results into a fine crystalline structure, that differs from the crystallographic structure of the original metal or alloy, through forming micrometric and submicrometric sub-grains in the coarse grain of the original material. The advantages of SPD on performance and mechanical properties through its ability to achieve deformations in the microstructure through fine grains, which reflects on the performance results of hardness and yield stress to saturation levels. However, SPD disadvantages are embodied mainly in the decreased ductility, decreasing the metal ability to undergo plastic deformation under stress.

The main aim of the current research is to test the effect of SPD through electric arc welding and shot peening on the mechanical and microstructure of ST37-2. It is

expected for these processes to affect the microstructure and homogeneity of the specimens, which leads to altering their mechanical properties. Six samples were prepared in order to test the mechanical properties and perform microstructure characterization.

Two Almen intensities were used A12-14 and A28-30. The surface roughness values showed substantial increases in Ra, Rq and Rz values between A12-14 and untreated ST37-2 samples, while a higher increase in roughness was achieved with A-23-30 shot peening. The tensile strength values indicate enhancements in yield strength and ultimate tensile strength values reaching up to 19.7% and 22.8% with CSP and SSP, respectively, while elongation decreased up to 27.2%, confirming the decrease in ductility with shot peening. Hardness of the alloy increased in treated samples, as well as changes in microstructure are indicated through XRF and XRD analyses. Deformation intensities are increased, as investigated through optical microscopy, while the layer thickness increase in the SSP case, in comparison with the CSP case, is observed in the FESEM study. Some data confirm the findings of the literature, while the research contribute into the literature with first time and original data.

Future research on subject is recommended to repeat the utilized test within this research and perform them on other grades of low carbon steel, including ST37-2, for comparison and reference. The fatigue test is recommended to be added to the methodology in order to be able to compare results with the majority of the studies, as well as form a comprehensive database for the alloy.

REFERENCES

[1] D. Llewellyn and R. Hudd, Steels: Metallurgy and Applications, 3rd ed., Oxford: Butterworth-Heinemann, 1998.

[2] I. E. Ahaneku, A. R. Kamal and O. A. Ogunjirin, "Effects of Heat Treatment on the Properties of Mild Steel Using Different Quenchants," *Frontiers in Science,* vol. 2, no. 6, pp. 153-158, 2012.

[3] M. K. Singh, "Application of Steel in Automotive Industry," *International Journal of Emerging Technology and Advanced Engineering,* vol. 6, no. 7, pp. 246-253, 2016.

[4] V. Sharma, R. Kumar, H. Singh, W. Ahmad and Y. Pratap, "A Review Study on uses of steel in construction," *International Research Journal of Engineering and Technology,* vol. 4, no. 4, pp. 1140-1142, 2017.

[5] L. Singh, R. A. Khan and M. L. Aggarwal, "Effect of shot peening on hardening and surface roughness of nitrogen austenitic stainless steel," *International Journal of Engineering Science and Technology,* vol. 2, no. 5, pp. 818-826, 2010.

[6] A. Kubit, M. Bucior, W. Zielecki and F. Stachowicz, "The impact of heat treatment and shot peening on the fatigue strength of 51CrV4 steel," *Procedia Structural Integrity,* vol. 2, pp. 3330-3336, 2016.

[7] Y. Ma, M. Yang, F. Yuan and X. Wu, "A Review on Heterogeneous Nanostructures: A Strategy for Superior Mechanical Properties in Metals," *Metals,* vol. 9, no. 598, 2019.

[8] M. Umemoto, Y. Todaka and K. Tsuchiya, "Formation of Nanocrystalline Structure in Steels by Air Blast Shot Peening," *Materials Transactions,* vol. 44, no. 7, pp. 1488-1493, 2003.

[9] O. Unal and E. Maleki, "Shot peening optimization with complex decision-making tool: Multi criteria decision-making," *Measurement,* vol. 125, pp. 133-141, 2018.

[10] D. Kumar, S. Idapalapati, W. Wang and S. Narasimalu, "Effect of Surface Mechanical Treatments on the Microstructure-Property-Performance of Engineering Alloys," *Materials (Basel),* vol. 12, no. 16, p. 2503, 2019.

[11] A. A. Dounde, C. Y. Seemiken and P. R. Tanpure, "Study of Shot Peening Process and Their Effect on Surface Properties: A Review," *International Journal of Engineering, Business and Enterprise Applications*, vol. 12, no. 2, pp. 104-107, 2015.

[12] M. Sledz, L. Bak, F. Stachowicz and W. Zielecki, "Analysis of the effect of shot peening on mechanical properties of steel sheets used as screener sieve materials," *Journal of Physics: Conference Series,* vol. 451, 2013.

[13] M. Chaib, A. Megueni, A. Ziadi, M. Guagliano and F. J. V. Belzunce, "Experimental study of the shot peening treatment effect on austenitic stainless steel," *International Journal of Materials and Product Technology,* vol. 53, no. 3/4, pp. 298-314, 2016.

[14] D. Cseh, V. Martinger and J. Lukacs, "Residual Stress Behavior in Hardened Shot Peened 42CrMo4 Specimens during Fatigue Load," *Materials Research Proceedings,* vol. 2, pp. 491-496, 2016.

[15] H. S. Ho, D. L. Li, E. L. Zhang and P. H. Niu, "Shot Peening Effects on Subsurface Layer Properties and Fatigue Performance of Case-Hardened 18CrNiMo7-6 Steel," *Advances in Materials Science and Engineering,* 2018.

[16] M. A. S. Torres and H. J. C. Voorwald, "An evaluation of shot peening, residual stress and stress relaxationon the fatigue life of AISI 4340 steel," *International Journal of Fatigue,* vol. 24, pp. 877-886, 2002.

[17] G. Rosenberg, "Effect of shot peening on fatigue properties of steel in different structural states," *Materials engineering,* vol. 18, pp. 68-72, 2011.

[18] W. F. Hosford, Iron and Steel, Cambridge: Cambridge University Press, 2012.

[19] H. D. Bowman, History and Development of the Steel Industry: Thesis, London: Forgotten Books, 2019.

[20] J. P. Dhal and S. C. Mishra, Material for Cryogenic Applications: Cryogenic Steel, Mauritius: LAP LAMBERT Academic Publishing, 2012.

[21] P. Warrian, A Profile of the Steel Industry: Global Reinvention for a New Economy (Industry Profiles Collection), New York: Business Expert Press, 2012.

[22] R. Holt and W. Holt, Modern Chemistry: Holt Modern Chemistry, New York: Holt, Rinehart and Winston, 2009.

[23] A. H. Cottrell, Introduction to Metallurgy, Los Angeles: Edward Arnold, 1967.

[24] P. C. Angelo and B. Ravisankar, Introduction to Steels: Processing, Properties, and Applications, Boca Raton, Florida: CRC Press, 2019.

[25] W. Smith and J. Hashemi, Foundations of Materials Science and Engineering, 5th ed., New York: McGraw-Hill Education, 2009.

[26] E. P. DeGarmo, J. T. Black and R. A. Kosher, DeGarmo's Materials and Processes in Engineering, Hoboken, New Jersey: Wiley, 2007.

[27] K. J. Pascoe, An Introduction to the Properties of Engineering Materials, New York: Van Nostrand Reinhold Company, 1976.

[28] H. Bhadeshia and R. Honeycombe, Steels: Microstructure and Properties, 4th ed., Oxford: Butterworth-Heinemann, 2017.

[29] R. W. K. Honeycombe, Steels: Microstructure and properties (Metallurgy and materials science), Russell Township: American Society for Metals, 1982.

[30] P. D. Harvey, Engineering Properties of Steel, Russell Township: ASM International, 1982.

[31] G. E. Totten, teel Heat Treatment: Metallurgy and Technologies, 2nd ed., Boca Raton: CRC Press, 2006.

[32] G. Krauss, Steels: Processing, Structure, And Performance, Russell Township: ASM International, 2005.

[33] K. Liverman, Alloy Steel: Features and Applications, New York: NY RESEARCH PRESS, 2015.

[34] A. Vosmaer, The Mechanical and Other Properties of Iron and Steel in Connection with Their Chemical Composition, South Yarra, Victoria: Leopold Classic Library, 2016.

[35] J. A. Sidawi and H. Khatib, "Evaluation of the Properties of S235JR Structural Carbon Steel in Lebanon," *Lebanese Science Journal,* vol. 3, no. 2, pp. 81-98, 2002.

[36] R. A. Rahbar and A. H. Zakeri, "Mechnical Properties and Corrosion Resistance of Normal Strength and High Strength Steels in Chloride Solution," *Journal of Naval Architecture and Marine Engineering,* vol. 7, pp. 94-100, 2010.

[37] A. Fadaei and H. Mokhtari, "Finite Element Modeling and Experimental Study of Residual Stresses in Repair Butt Weld of ST-37 Plates," *IJST, Transactionsof Mechanical Engineering,* vol. 39, no. M2, pp. 291-307, 2015.

[38] O. Turcan, D. Comeaga, O. Dontu and I. Voiculescu, "Improvement of Low Carbon Steel ST37-2 by Laser Surface Alloying with Metallic Powders," *Advanced Materials Research,* Vols. 816-817, pp. 250-254, 2013.

[39] M. Aberkane and M. O. Ouali, "Fracture characterization of ST37-2 thin metal sheet with experimental and numerical methods," *Key Engineering Materials,* vol. 473, pp. 396-403, 2011.

[40] S. Djebali, S. Larbi and A. Bilek, "Tenacity of Sheet Steel ST37-2 by the Essential Work of Fracture Method," *Procedia Engineering,* vol. 114, pp. 306-313, 2015.

[41] M. Ebrahimnia, M. Goodarzi, M. Nouri and M. Sheikhi, "Study of the effect of shielding gas composition on the mechanical weldproperties of steel ST 37-2 in gas metal arc welding," *Materials and Design,* vol. 30, pp. 3891-3895, 2009.

[42] O. Turcan, O. Dontu, J. L. Ocana Moreno, I. Voiculescu and I. M. Vasile, "Aspects Regarding the Possibility of Increasing Hardness on a Low Carbon Steel ST37-2 by Surface Treatment with CO2 Laser," *UPB Scientific Bulletin, Series B: Chemistry and Materials Science,* vol. 76, no. 2, 2014.

[43] N. Chhabra and V. Bansal, "A Review of Effect of Shielding Gases Mixture on Welded Joint Properties of Low Carbon Steel in Mig/Mag Welding Process," *International Journal of Scientific Research,* vol. 5, no. 1, pp. 34-36, 2016.

[44] R. Rakhmetov, S. A. Krainov, M. N. Nazarova and A. N. Tsenev, "Research of main gas pipelilne (steels X65, X60, 17G1S) susceptibility to stress corrosion cracking, hydrogen uptake and ST 37-2 steel fatigue testing," *IOP Conf. Series: Earth and Environmental Science,* vol. 194, 2018.

[45] U. Sonmez and V. Ceyhun, "Investigation of mechanical and microstructural propertiesof S 235 JR (ST 37-2) steels welded joints with FCAW," *Kovove Materialy - Mettalic Materials,* vol. 52, pp. 57-63, 2014.

[46] S. Karthick, S. Muralidharan and V. Saraswathy, "Corrosion performance of mild steel and galvanizediron in clay soil environment," *Arabian Journal of Chemistry,* vol. 13, pp. 3301-3318, 2020.

[47] H. S. Link and R. J. Schmtt, "Iron, Carbon Steel, and Alloy Steel. Materials of Construction Review," *Industrial & Engineering Chemistry,* vol. 53, no. 7, pp. 590-595, 1961.

[48] F. Moerman and E. Partington, "Materials of construction for food processing euipment and service: requirements, strengths and weaknesses," *Journal of Hygienic Engineering and Design,* vol. 6, pp. 10-37, 2014.

[49] Mandal, Steel Metallurgy: Properties, Specifications and Applications, 1st ed., New York: McGraw-Hill Education, 2015.

[50] J. R. Davis, Ed., Metals Handbook, 2nd ed., USA: ASM International, 1998.

[51] E. T. Turkdogan, G. J. W. Kor, L. S. Darken and R. W. Gurry, "Sulfides and oxides in Fe−Mn alloys: Part I. Phase relations in Fe−Mn−S−O system," *Metallurgical Transactions,* vol. 2, p. 1561, 1971.

[52] A. Nicholson and J. D. Murray, "Surface hot shortness in low carbon steel," *The Journal of the Iron and Steel Institute,* vol. 203, p. 1007, 1965.

[53] W. Crafts and J. L. Lamont, "Effect of some elements on hardenability," *Transactions of the Metallurgical Society of AIME,* vol. 158, p. 157, 1944.

[54] C. L. Jenney and A. O'Brien, Eds., Welding Handbook, 9th ed., vol. 1, Miami: American Welding Society, 2001.

[55] C. G. de Abdres, F. G. Caballero, C. Capdevila and H. K. D. H. Bhadeshia, "Modelling of kinetics and dilatometric behavior of non-isothermal pearlite-to-austenite transformation in an eutectoid steel," *Scripta Materialia,* vol. 39, no. 6, pp. 791-796, 1998.

[56] P. Gomez, F. Reyes, J. Gutierrez and G. Plascencia, "Assessment of thermochemical data on steel deoxidation," *Revista de Metalurgia,* vol. 45, no. 4, pp. 305-316, 2009.

[57] A. Monsalve, A. Artigas and D. Celentano, "Effect of aluminium nitride precipitation on recrystallisation kinetic in low carbon batch," *Revista de Metalurgia (Metallurgy Magazine),* vol. 41, pp. 340-350, 2005.

[58] J. M. Cabrera, A. Al Omar, J. J. Jonas and J. M. Prado, "Modeling the flow behavior of a medium carbon microalloyed steel under hot working conditions," *Metallurgical and Materials Transactions A,* vol. 28, no. 11, pp. 2233-2244, 1997.

[59] L. F. Zagonel, J. Bettini, R. L. O. Basso, P. Paredez, H. Pinto, C. M. Lepienski and F. Alvarez, "Nanosized precipitates in H13 tool steel low temperature plasma nitriding," *Surface and Coatings Technology,* vol. 207, pp. 72-78, 2012.

[60] G. C. Ortega, N. C. Vazquez, M. P. Martinez, R. B. Del Cerro and M. C. Cebrian, "Influence of the austenite-martensite transformation on the dimensional stability of a new tool steel alloyed with niobium (0.08%) and vanadium (0.12%)," *Revista de Metalurgia (Metallurgy Magazine),* vol. 50, no. 3, p. 018, 2014.

[61] C. Fossaert, G. Rees, T. Maurichx and H. K. D. H. Bhadeshia, "The effect of niobium on the hardenability of microalloyed austenite," *Metallurgical and Materials Transactions A,* vol. 26, pp. 21-30, 1995.

[62] N. K. Balliger and R. W. K. Honeycombe, "The effect of nitrogen on precipitation and transformation kinetics in vanadium steels," *Metallurgical Transactions A,* vol. 11, pp. 421-429, 1980.

[63] M. Free, "Important Machining Factors of Carbon Steels," PM Production Machining, 22 March 2006. [Online]. Available: https://www.productionmachining.com/blog/post/important-machining-factors-of-carbon-steels. [Accessed 05 January 2020].

[64] E. C. Bain, The Alloying Elements in Steel, Russell Township: ASM International, 1939.

[65] O. B. Owolabi, S. C. Aduloju, C. S. Metu, C. E. Chukwunyelu and E. C. Okwuego, "Evaluation of the effects of welding current on mechanical properties of welded joints between mild steel and low carbon steel," *American Journal of Materials Science and Application,* vol. 4, no. 1, pp. 1-4, 2016.

[66] M. A. Bodude and I. Momohjimoh, "Studies on Effects of Welding Parameters on the Mechanical Properties of Welded Low-Carbon Steel," *Journal of Minerals and Materials Characterization and Engineering,* vol. 3, pp. 142-153, 2015.

[67] Z. Bounerzoug, C. Derfouf and T. Baudin, "Effect of Welding on Microstructure and Mechanical Properties of an Industrial Low Carbon Steel," *Engineering,* vol. 2, pp. 502-506, 2010.

[68] Husaini, N. Ali, J. K. Hamza and S. E. Sofyan, "Effects of welding on the change of microstructure and mechanical properties of low carbon steel," *Materials Science and Engineering,* vol. 523, 2019.

[69] D. Sumardiyanto and S. E. Susilowati, "Effect of WeldingParameters on Mechanical Properties of Low Carbon Steel API 5L Shielded Metal Arc Welds," *American Journal of Materials Science,* vol. 9, no. 1, pp. 15-21, 2019.

[70] D. Kumar, S. Idapalapati, W. Wang and S. Narasimalu, "Effect of Surface Mechanical Treatments on theMicrostructure-Property-Performance ofEngineering Alloys," *Materials,* vol. 12, 2019.

[71] L. Wagner, Shot Peening, Hoboken, New Jersey: Wiley-VCH, 2003.

[72] MIC, Shot-Peening Applications, 6th ed., New Jersey: Metal Improvement Company, 1980.

[73] J. Champaigne, Shot peening: theory and application, Chicago: IITT-International, 1991.

[74] B. Bhuvaraghan, S. M. Srinivasan and B. Maffeo, "Optimization of the fatigue strength of materials due to shot peening : A Survey," *International Journal of Structural Changes in Solids - Mechanics and Applications,* vol. 2, no. 2, pp. 33-63, 2010.

[75] A. Ampaiboon, O. U. Lasunon and B. Bubphachot, "Optimization and Prediction of Ultimate Tensile Strength in Metal Active Gas Welding," *The Scientific World Journal,* 2015.

[76] R. Ranji and A. H. Zakeri, "Mechanical Properties and Corrosion Resistance of Normal Strength and High Strength Steels in Chloride Solution," *Journal of Naval Architecture and Marine Engineering,* vol. 7, pp. 93-100, 2010.

[77] I. Karademir, O. Unal, S. Ates, H. Gokce and M. Gok, "Effect of Severe Plastic Deformation on Wear Properties of Aluminum Matrix Composites," *Acta Physica Polonica A,* vol. 131, no. 3, pp. 487-489, 2017.

[78] O. Unal, I. Zulcic, R. Varol, I. Karademir and S. Ates, "Novel type shot peening applications on railway axle steel," *Journal of Mineral Metal and Material Engineering,* vol. 2, pp. 1-5, 2016.

[79] O. Unal and R. Varol, "Surface nanostructuring of AISI 1017 by severe shot peening," *Research and Reports on Metals,* vol. 1, pp. 1-4, 2017.

[80] O. Unal, A. C. Karaoglanli, Y. Ozgurluk, K. M. Doleker, E. Maleki and R. Varol, "Wear behavior of severe shot peened and thermally oxidized commercially pure titanium," *Engineering Design Applications,* vol. 5, pp. 461-470, 2019.

[81] M. A. Omari, H. M. Mousa, F. M. Al-Oqla and M. Aljarrah, "Enhancing the surface hardness and roughness of engine blades using the shot peening process," *International Journal of Minerals, Metallurgy and Materials,* vol. 26, no. 8, pp. 999-1004, 2019.

[82] W. Liu, J. Ding, P. Zhang, C. Zhai and W. Ding, "Effect of Shot Peening on Surface Characteristics and Fatigue Properties of T5-Treated ZK60 Alloy," *Materials Transactions,* vol. 50, no. 4, pp. 791-798, 2009.

[83] A. Thakur and G. Aregawi, "Effect of Heat Treatment on Mechanical Properties and Microstructure of ST 37-2 Rear Trailing Arm," *International Journal of Current Engineering and Technology,* vol. 9, no. 1, pp. 80-91, 2019.

[84] E. Maleki and G. H. Farrahi, "Modelling of Conventional and Severe Shot Peening Influence on Properties of High Carbon Steel via Artificial Neural Network," *International Journal of Engineering,* vol. 30, no. 11, pp. 382-393, 2017.

[85] M. Yazdani, M. R. Toroghinejad and S. M. Hashemi, "Investigation of Microstructure and Mechanical Properties of St37 Steel-Ck60 Steel Joints by Explosive Cladding," *Journal of Materials Engineering and Performance,* vol. 24, pp. 4032-4043, 2015.

[86] F. O. Sonmez and A. Demir, "Analytical relations between hardness and strain for cold formed parts," *Journal of Materials Processing Technology,* vol. 186, pp. 163-173, 2007.

[87] A. B. M. Helaluddin, R. S. Khalid, M. Alaama and S. A. Abbas, "Main Analytical Techniques Used for Elemental Analysis in Various Matrices," *Tropical Journal of Pharmaceutical Research,* vol. 15, no. 2, pp. 427-434, 2016.

[88] M. I. Mohamed, "Studies of the Properties and Microstructure of Heat Treated 0.27% C and 0.84% Mn Steel," *Engineering, Technology and Applied Science Research (ETASR),* vol. 8, no. 5, pp. 3484-3487, 2018.

[89] S. H. Abro, A. Chandio, A. R. Jamali and S. A. Shah, "Influence of Austenite Phase Transformation on Existing Microstructure of Low C-Mn Steel," *Engineering, Technology & Applied Science Research (ETASR),* vol. 8, no. 6, pp. 3525-3529, 2018.

APPENDIX A.

FESEM IMAGES

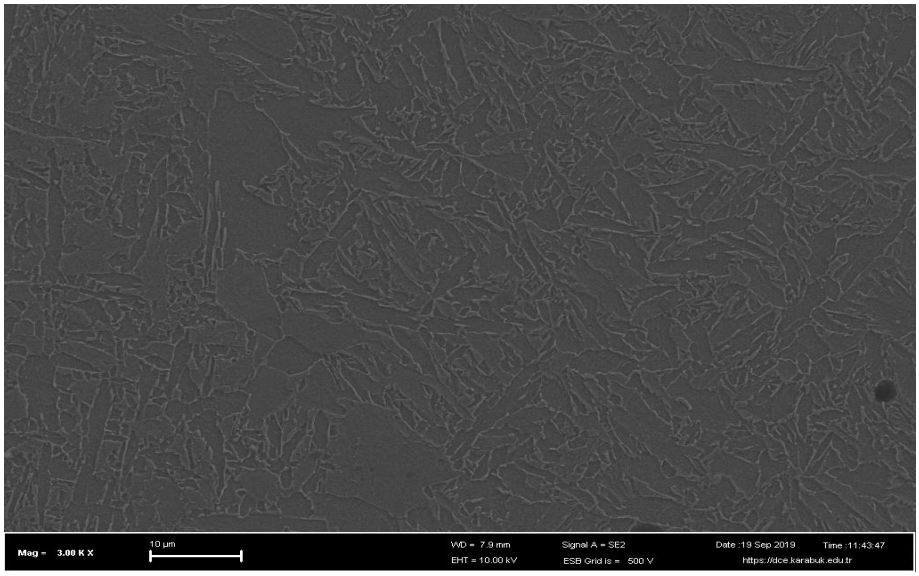

Figure A.1. FESEM images and thickness of the plastic deformed layer of shot peened specimens ST 37-2 (Magnification at 3.00 KX).

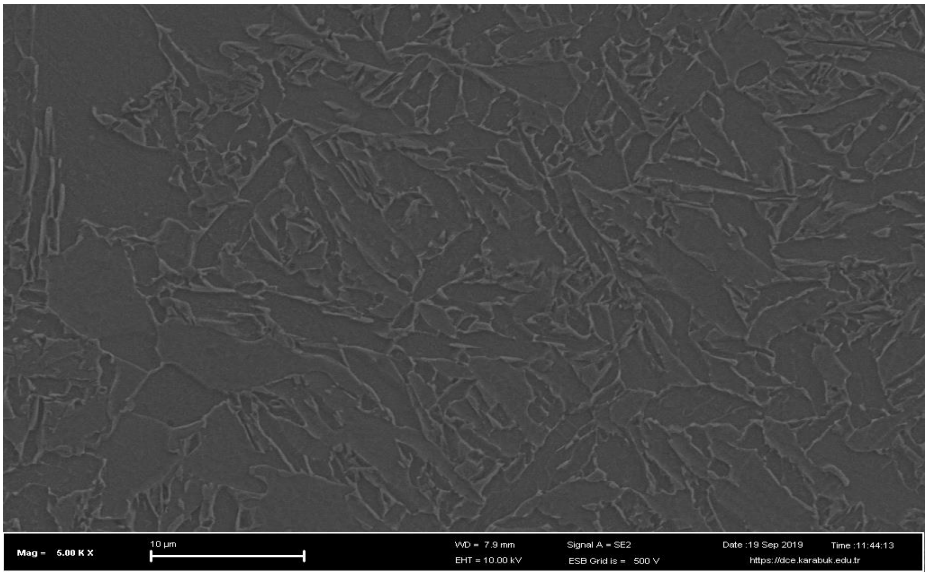

Figure A.2. FESEM images and thickness of the plastic deformed layer of shot peened specimens ST 37-2 (Magnification at 5.00 KX).

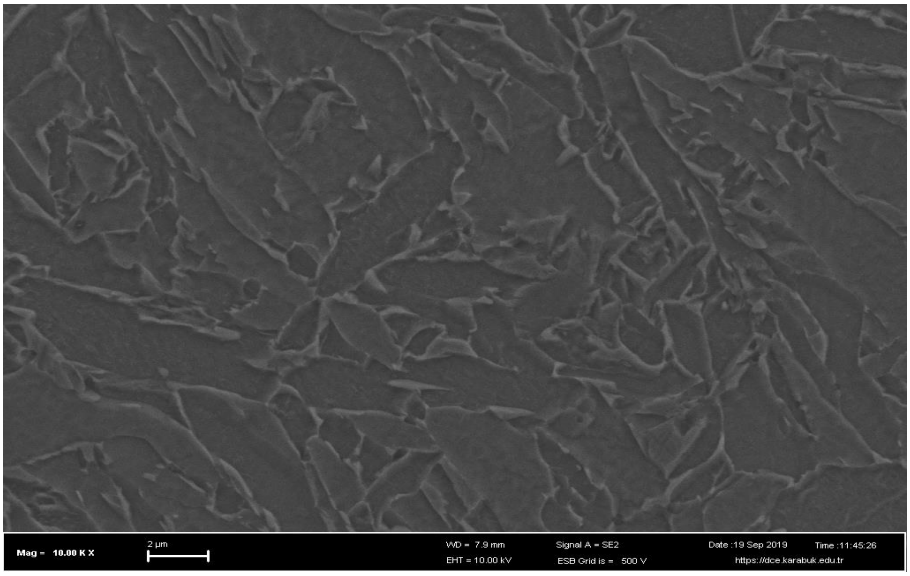

Figure A.3. FESEM images and thickness of the plastic deformed layer of shot peened specimens ST37-2 (Magnification at 10.00 KX).

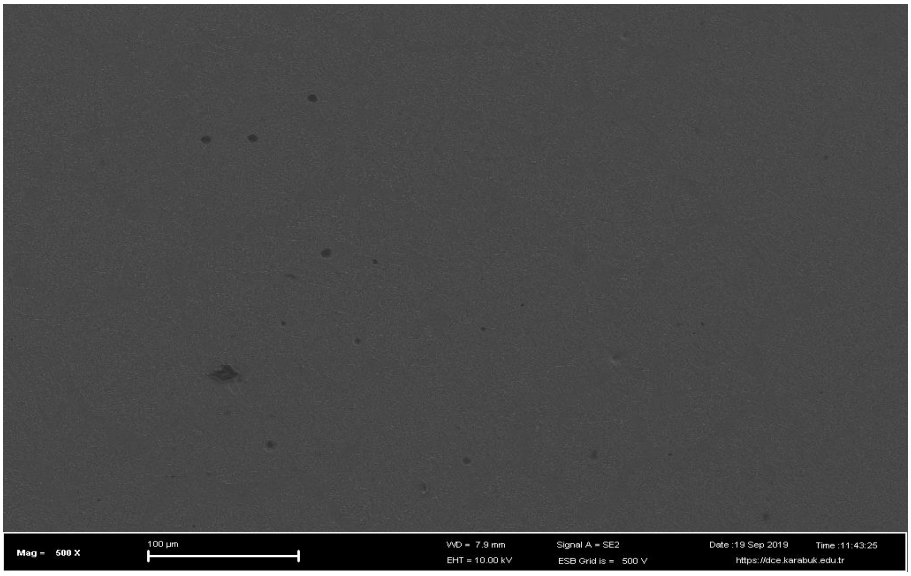

Figure A.4. FESEM images and thickness of the plastic deformed layer of shot peened specimens ST 37-2 (Magnification at 500 X).

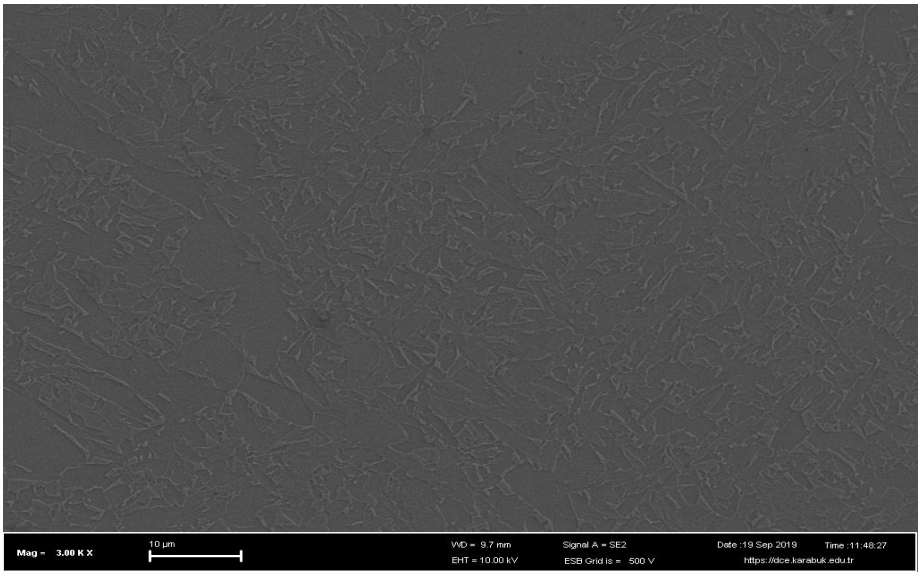

Figure A.5. FESEM images and thickness of the plastic deformed layer of shot peened specimen SSP (A28-30) (Magnification at 3.00 KX).

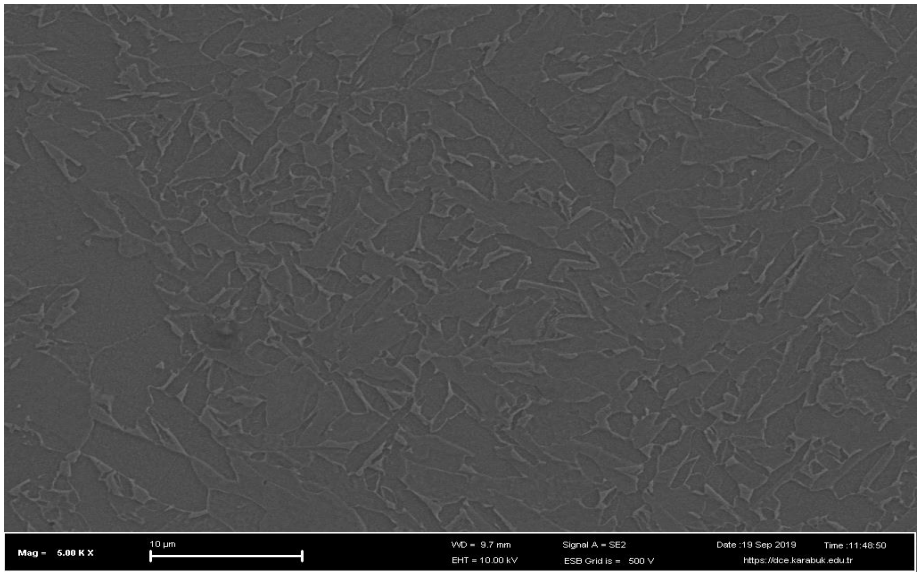

Figure A.6. FESEM images and thickness of the plastic deformed layer of shot peened specimen SSP (A28-30) (Magnification at 5.00 KX).

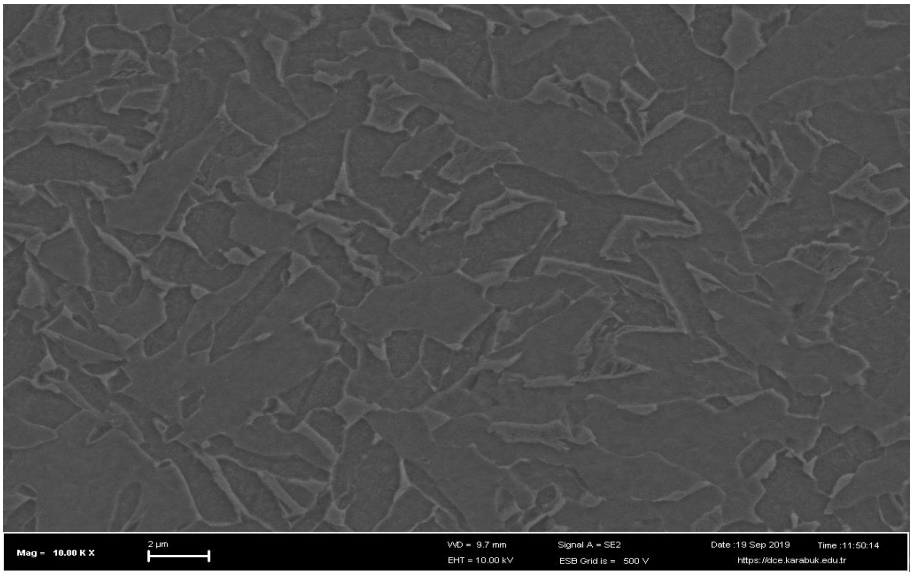

Figure A.7. FESEM images and thickness of the plastic deformed layer of shot peened specimen SSP (A28-30) (Magnification at 10.00 KX).

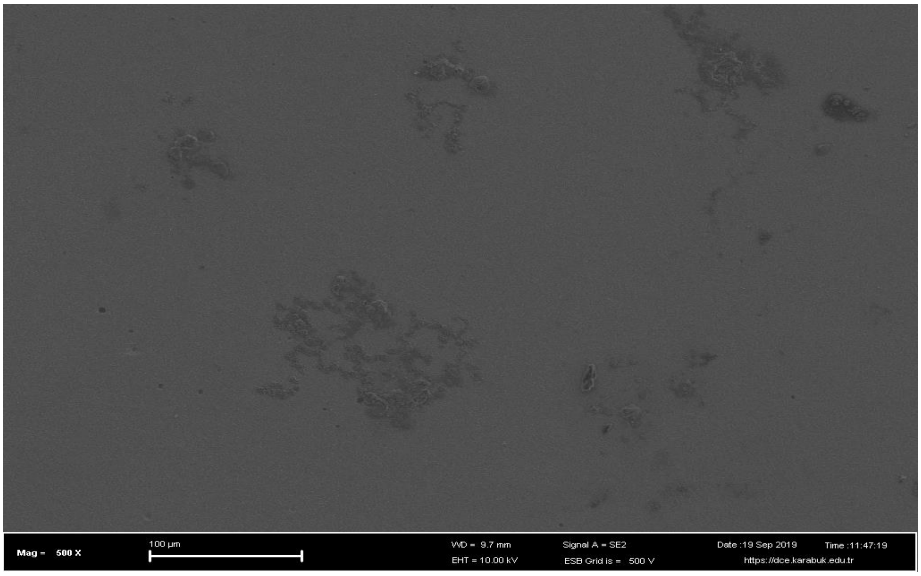

Figure A.8. FESEM images and thickness of the plastic deformed layer of shot peened specimen SSP (A28-30) (Magnification at 500 X).

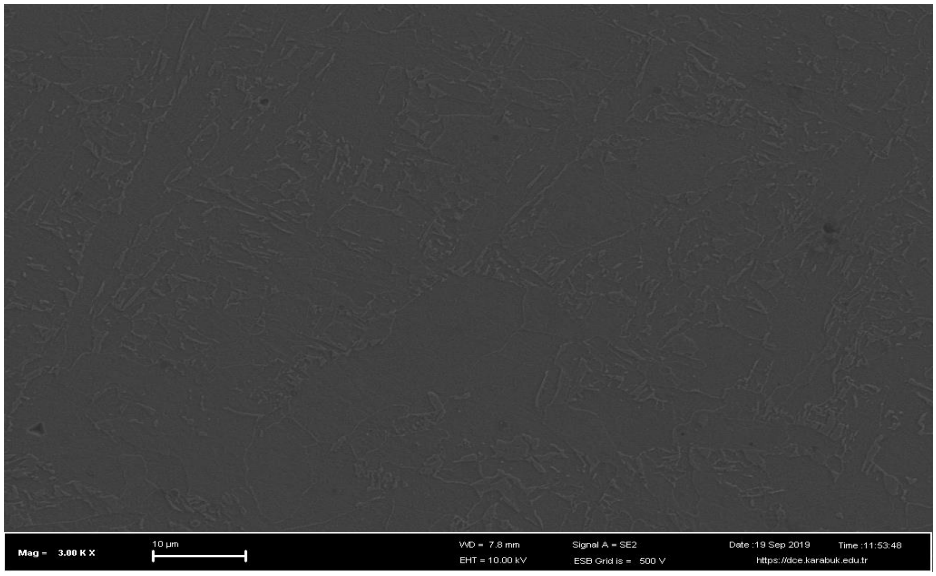

Figure A.9. FESEM images and thickness of the plastic deformed layer of shot peened specimen CSP (A12-14) (Magnification at 3.00 KX).

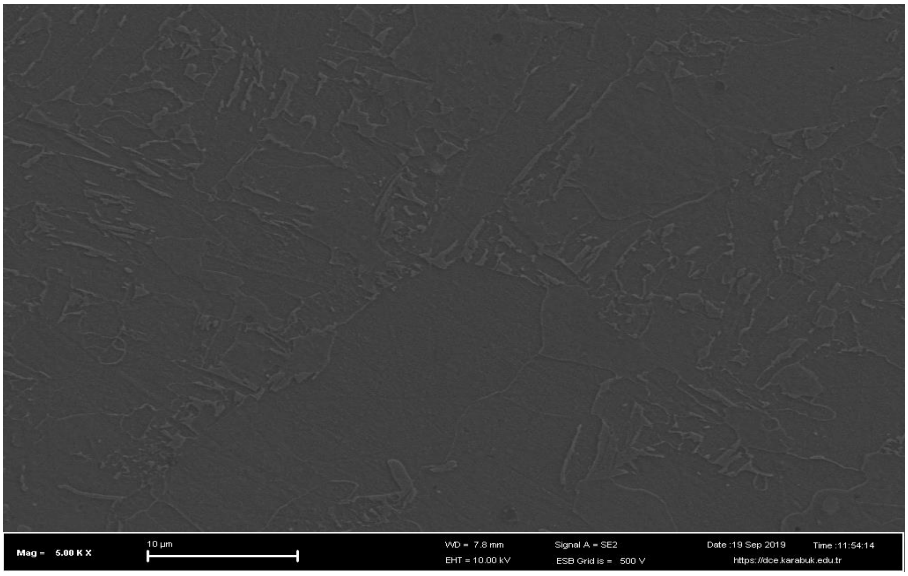

Figure A.10. FESEM images and thickness of the plastic deformed layer of shot peened specimen CSP (A12-14) (Magnification at 5.00 KX).

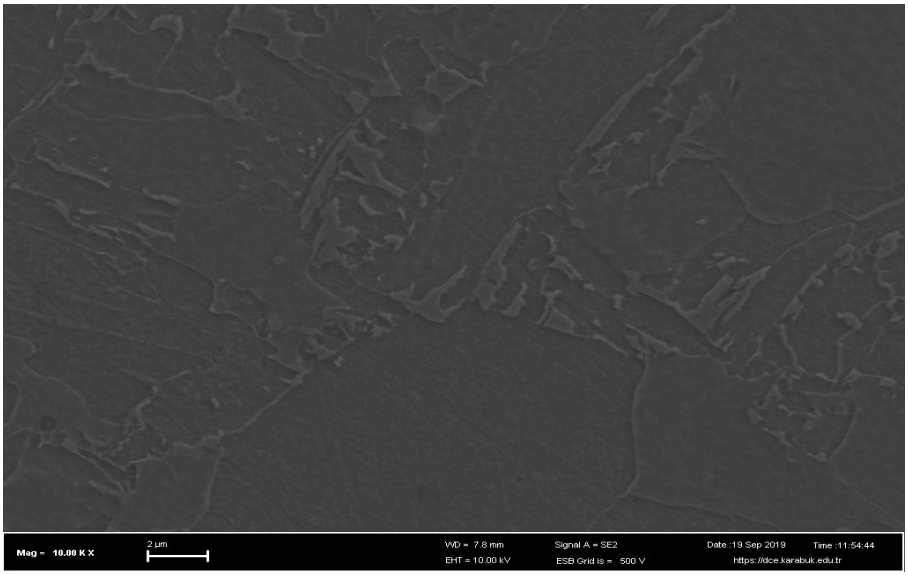

Figure A.11. FESEM images and thickness of the plastic deformed layer of shot peened specimen CSP (A12-14) (Magnification at 10.00 KX).

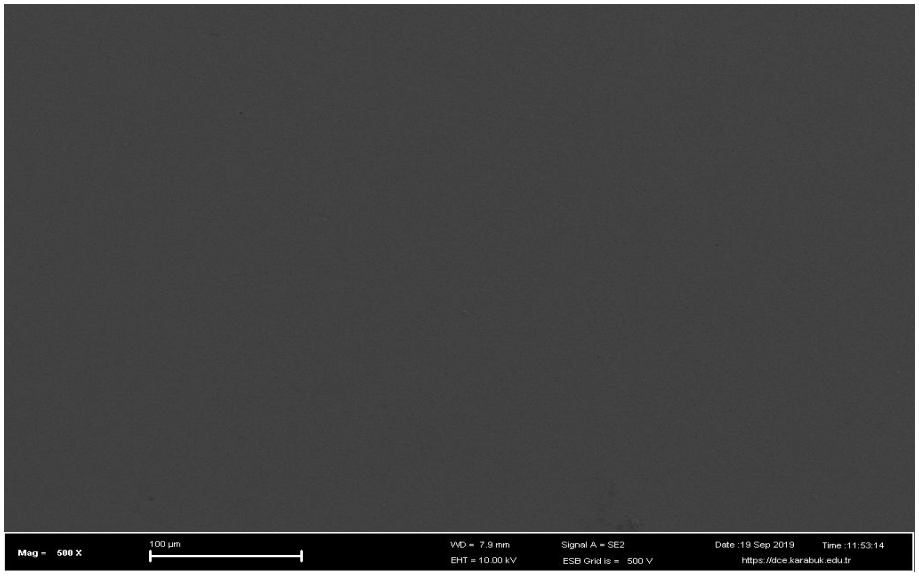

Figure A.12. FESEM images and thickness of the plastic deformed layer of shot peened specimen CSP (A12-14) (Magnification at 500 X).

RESUME

Abubaker H. Almabruk SAHHAL was born in Sarman, Libya in 1971. He completed his primary education in Sidi Khalifa School in Tripoli, and his preparatory and secondary education in Sarman city school. He started his university education in the department of mechanical engineering of the Higher Institute for Comprehensive Occupations with a specialty in power in 1995. He worked as a trainer in the Intermediate Institute for Mechanical Engineering until 1996 and as a workshop trainer in the Higher Institute of Marine Sciences until 2001. He completed his Masters in mechanical engineering at the University of Applied Sciences, Germany. He is currently completing his PhD in Mechanical Engineering at Karabük University, Turkey.

CONTACT INFORMATION

Address : Sarman, Libya
E-mail : abubaker_ahmad@yahoo.de